ISSN 0016-8521, Geotectonics, 2010, Vol. 44, No. 2, pp. 176–202. © Pleiades Publishing, Inc., 2010.

Study of the Cuban Fractures[1]

M. O. C. Rodriguez and D. Córdoba

Departamento de Física de la Tierra y Astrofísica I. Facultad de Ciencias Físicas, Universidad Complutense de Madrid. Ciudad Universiiaria, s/n, 28040 Madrid

Received July 11, 2008, in final form November 6, 2009

Abstract—With the help of aerial photographs, satellite photographs and imageries, contour maps, geological and geomorphological information (personal correspondence and unpublished works), geophysical regional data, and field work, it has been possible to map a network of fractures, alignments, and faults in 26 areas (distinguishing them quantitatively and hierarchically). Links with known regional structures were also studied. Interpretation of the linear relief elements confirms the very different density, dimensions, strikes, and function of the fracturation and also, from a microtectonic perspective, explains the activity of some active faults better. It has confirmed some previous results and improved on others; for example, the Oriente fault which is the most active in Cuba with two segments (Western: Cabo Cruz—Santiago de Cuba; Eastern: Santiago de Cuba—Punta de Maisí, the Western fault being the most active); the Nortecubana fault, forming the northern limit of the Cuban megablock, and divided into three segments; and the Cauto–Nipe fault, forming the limit of the neotectonic units, presenting two segments with three seismoactive knots.

DOI: 10.1134/S0016852110020068

INTRODUCTION

Tectonic studies have been made of Cuba (Fig. 1) to a varied extent and using several methods [12], and the data and results of these geological studies have formed the fundamental base for geological and geophysical investigations towards the end of the 20 th century [1–6]. Additionally, aerial photographs, satellite photographs and imageries, and topographic maps have permitted several authors to create a heterogeneous data base of fracturament, and have facilitated the development of several maps and schemes on different scales for the entire Cuban territory as a whole, and some zones in particular. However, the obtained results differ among themselves, even for some of the principal fault zones [24].

Cotilla et al. [23] suggested that the study of the neotectonic fractures in Cuba had not been satisfactory, arguing that it was essential to carry out a spatial–temporal study of the fracture systems in order to explain their formation mechanisms. Therefore, [18] proposed and presented the first study of neotectonic kinematics with a stress tensor in Eastern Cuba. Later, [16] obtained another tensor for Western Cuba.

The main objectives of the present research are two folds; to study active tectonics in some Cuban areas, on the basis of aerial photographs, satellite imageries and photographs, and available geological–geomorphological data; and also to study the morphostructural differentiation of 26 zones in Cuba (Table 1) (Fig. 2) based on the characteristics of the fluvial network and fracturing. All the information, its processing and manipulation, and the obtained results were supported by GIS [17].

DATA OF RELIEF, GEOLOGY, AND TECTONICS OF CUBA

Cuba is an archipelago (110922 km^2) located in the Caribbean (Fig. 1). It is the largest island in the Greater West Indies arch. Linear extension is 1256.20 km with a coastal perimeter of 5745.92 km (3208.81 and 2537.11 km on the northern coast and the southern coast, respectively) [39]. Its insular platform (~68000 km^2) completely surrounds the archipelago with a depth that varies from ~10 to ~55 m, and where abrasive and abrasive-denudative plains predominate. The platform has some sub-areal forms such as scarps, fluvial channels and depressions comprising different geometry, practically all of which are composed of calcareous formations [41]. The insular slope is a tectonic structural type step of some 5 km in depth forming a limit with the deeper zones (troughs and oceanic depressions).

J.L. Díaz [30] states that the present-day relief of Cuba is the result of the interaction of endogenous and exogenous processes in the North American and Caribbean regions. Climatic elements (tropical zone humidity) and geodinamic elements (contact with the Caribbean and North America plates) are heterogeneous. It has also been established that towards the end of the Paleogene in Cuba, vertical movements were initiated and compressive movements came to an end. In this way, the Alpine structures in this region were formed, which, together with the rest of the territory, were later subjected to the influence of other vertical

[1] The article is published in the original.

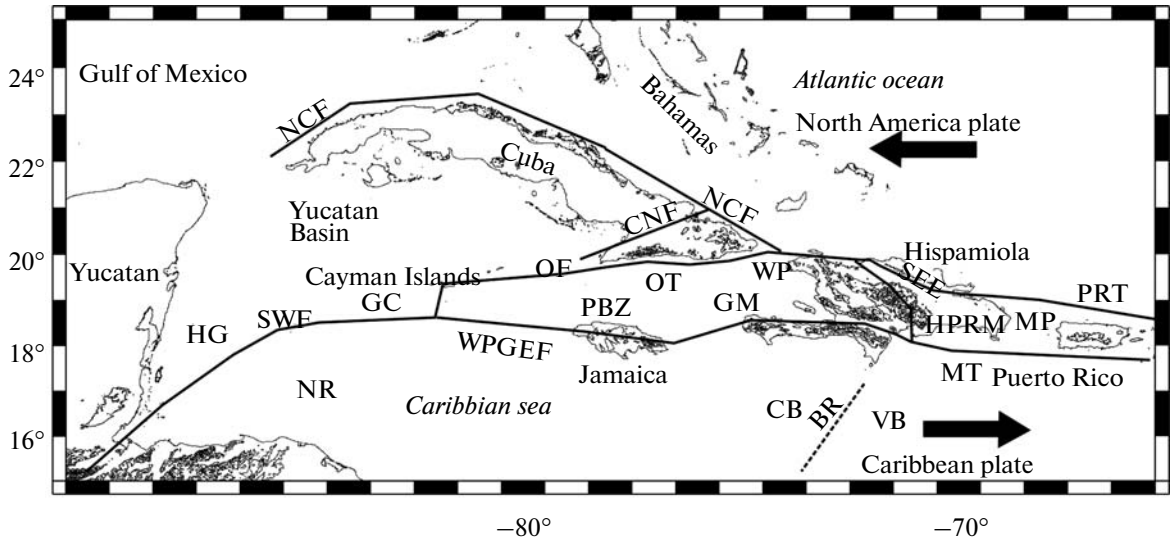

Fig. 1. Tectonic scheme of the Caribbean.

Heavy black arrows show the sense of the plate movements. With a set of points is the ridge structure: BR—Beata, NR—Nicaragua.

1—the main faults: CNF—Cauto–Nipe, NCF—Nortecubana, OF—Oriente, SEF—Septentrional, SWF—Swan, WPGEF—Walton–Platain Garden–Enriquillo; 2—passages: MP—Mona; WP—Windward; 3—islands: Cuba, Hispaniola, Jamaica, Puerto Rico; 4—basin: CB—Colombia, VB—Venezuela; 5—microplates: GM—Conave, HPRM—Hispaniola—Puerto Rico; 6—troughs: MT—Muertos, OT—Oriente, PRT—Puerto Rico, HG—Honduras-Guatemala, GC—crust generation centre.

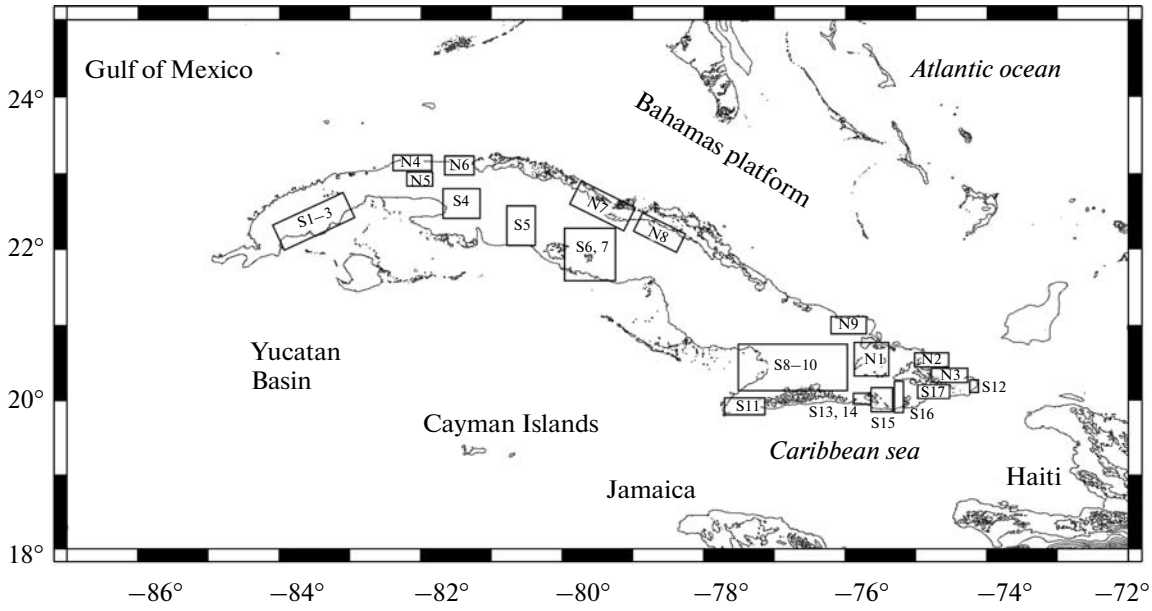

Fig. 2. Research areas (see Table 1).

pushes. Throughout the Upper Oligocene–Middle Miocene there was a period of general tectonic stability, with the formation and development of sedimentary basins, fed by the elevated bordering zones. From this period, one very reduced part of an ample surface of planation remains in present day elevations. This surface was fragmented as a consequence of endogenous processes at the end of the Miocene, causing blocks of different heights to rise, which now constitute the present-day Cuban neoplane [39].

The Cuban crust is split into two large geologically superimposed mosaics, corresponding to different stages of geological development: a folded belt and a neoautochthonous [53]. The neoautochthonous comprises the period from the Upper Eocene (upper part) to the Recent, where vertical oscillatory motions pre-

Table 1. Research areas

No.	Denomination	Locality, Province	Neotectonic Unit	Morpnotectonic type	Relief type	Watershed slope	Vertical tendency	Field stations	Faults
S1–3	San Cristóbal	San Cristóbal, Pinar del Río	Western	Macroblock	Plain	South	Downtrow	86	G
S4	Torriente	Torriente—J. Grande, Matanzas	Western	Mesoblock	Plain	South	Uplift	27	CH, HC
S5	Cienfuegos	Cienfuegos, Cienfuegos	Western	Mesoblock	Plain	South	Uplift	31	HC
S6–7	Trinidad	Trinidad, Sancti Spiritus	Western	Mesoblock	Plain	South	Uplift	44	LT
S8–10	Bayamo	Bayamo–Manzanillo, Granma	Eastern	Macroblock	Plain	South	Downtrow	65	CN
S11	Cabo Cruz	Cabo Cruz—Pilón, Granma	Eastern	Mesoblock	Plain	South	Uplift	16	CN, O
S12	Maisí	Maisí, Guantánamo	Eastern	Mesoblock	Plain	South	Uplift	16	NC, O
S13–14	Santiago	Stgo. de Cuba, Stgo. de Cuba	Eastern	Mesoblock	Plain	South	Uplift	38	O
S15	Baconao	Baconao, Santiago de Cuba	Eastern	Mesoblock	Plain	South	Uplift	42	B, O
S16	Guantánamo	Guantánamo, Guantánamo	Eastern	Mesoblock	Plain	South	Uplift	21	O
S17	San Antonio	San A. del Sur, Guantánamo	Eastern	Mesoblock	Plain	South	Uplift	20	O
N1	Mayarí	Mayarí, Holguín	Eastern	Mesoblock	Heigth	North	Uplift	40	CN, NC
N2	Moa	Moa, Holguín	Eastern	Mesoblock	Mountainous	North	Uplift	37	NC
N3	Baracoa	Baracoa, Guantánamo	Eastern	Mesoblock	Mountainous	North	Uplift	42	NC
N4	Habana	La Habana, C. de La Habana	Western	Macroblock	Plain	North	Uplift	25	HC, NC
N5	San José	San J. de las Lajas, La Habana	Western	Mesoblock	Plain	North	Uplift	20	G, HC
N6	Matanzas	Matanzas, Matanzas	Western	Mesoblock	Plain	North	Uplift	19	H, NC
N7	Remedios	Remedios–Caibarién, Las Villas	Western	Mesoblock	Plain	North	Downtrow	25	LV, NC
N8	Esmeralda	Esmeralda, Ciego de Avila	Western	Mesoblock	Plain	North	Uplift	17	C
N9	Gibara	Gibara–Bariay, Holguín	Western	Mesoblock	Heigth	North	Uplift	25	NC

Note: B—Baconao, C—Cubitas, CH—Cochinos, CN—Cauto–Nipe, G—Guane, H—Hicacos, HC—Habana–Cienfuegos, LT—La Trocha, LV—Las Villas, NC—Nortecubana, O—Oriente.

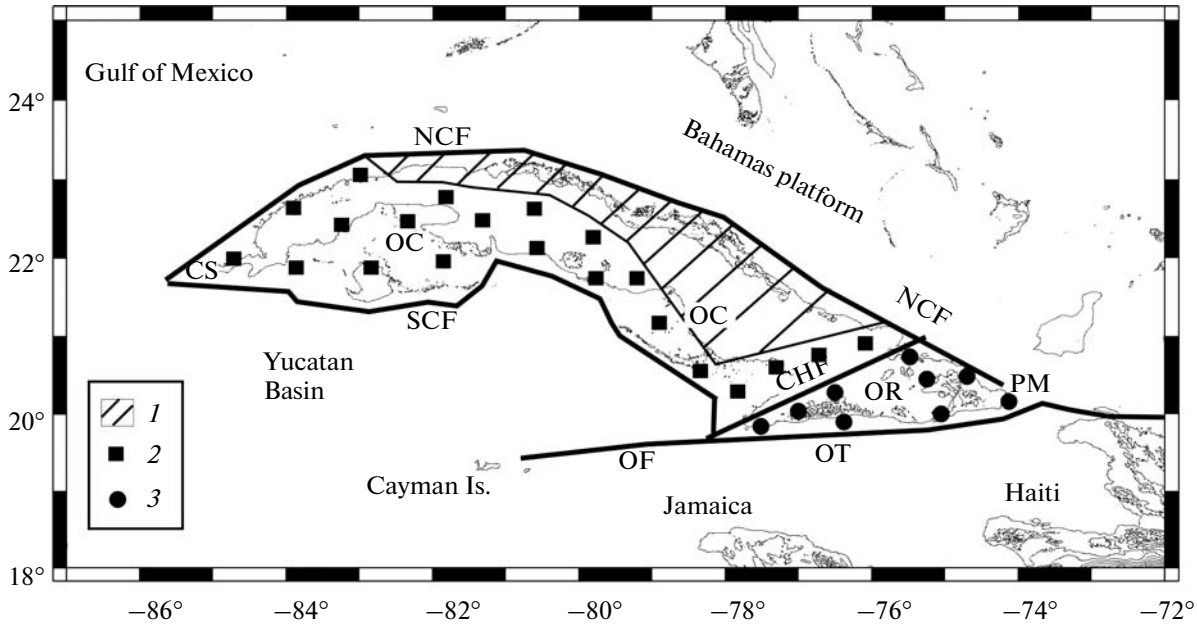

Fig. 3. Cuban megablock.

Heavy black line—Faults: CNF—Cauto–Nipe, NCF—Nortecubana, OF—Oriente, SCF—Surcubana). Neotectonic Unit: OC—Western, OR—Eastern. Crust type: 1—post-orogenic complex, 2—orogenic complex, 3—volcanic arc complex. Localities: CS—Cabo de San Antonio, PM—Punta de Maisí.

dominate, with subordinate left hand strike-slip (NE–SW strike) faults, probably related to transpressure exercised along the northern margin of the Caribbean plate. At the same time, basins were formed along the deformed belt with klastic and carbon deposits, but without magmatic activity. In spite of the fact that three main stages in the evolution of the basins are clearly identifiable, each of them with a complete cycle of transgression–regression, upliftings dominate the general tectonic evolution. The neoautochthonous stage began with the activation of the Bartlett–Cayman trough, with its pull apart system, when convergent tectonic processes in the Caribbean plate changed positions successively and progressively east [71].

NOTES ON THE CUBAN NEOTECTONIC UNITS

According to the results of Cotilla et al. [23], the Cuban megablock comprises two neotectonic units (NU), the Western unit (We) and the Eastern unit (Ea), which are separated by a transverse-diagonal fault (NE–SW), called the Cauto–Nipe (Fig. 3). The NUWe extends from the area surrounding the Cabo de San Antonio (extreme west of Cuba) to the Cauto–Nipe depression, and is characterised by interior plate type seismicity. The plains cover a greater area than the peaks, and maximum elevation is less than for the other Unit. Relief is less pronounced. The principal watershed of first order does not present significant irregularities along its course between the Cabo de San Antonio (in the west) and the Punta de Maisí (in the east). The most important rivers are of a lesser order than in the NUEa. Sectors of neotectonic rising are considerably less numerous than in the east, and there are large areas where they do not even appear. These movements are all contained in the Guamuhaya Mountain Range (in the south and centre of Cuba), slightly exceeding 1000 m in height, whilst the rest of the Western territory is considerably lower.

The NUWe displays relatively homogeneous neotectonic activity from the Upper Eocene to the present, although new uplifting movements in the raised blocks comprising Guamuhaya and the Isla de la Juventud were not initiated after the Maestrichtian, and for those comprising Guaniguanico (the most western Mountain Range) and the north of Central Cuba, after the Middle Eocene. A system of blocks was formed and the fault system radically modified, in particular, two extensive and heterogeneous active fault systems in the marine section (Nortecubana and Surcubana), which constitute the northern and southern limits, respectively, of the Cuban megablock. In contrast, the NUEa has a much greater surface area than the NUWe, with a much more pronounced relief in direct contact with the Caribbean and North American plates along the entire length of its southeast edge (the Oriente fault). To the south is the Oriente trough, with acute seismic activity and earthquakes of up to 9 degrees of intensity, MSK (Medvedev–Sponheur–Karnick seismic scale) [21]. Two branches of the principal watershed have been defined in this Unit, an exception for the Caribbean as it is for the La Española (with 4 branches). The extent of the vertical neotec-

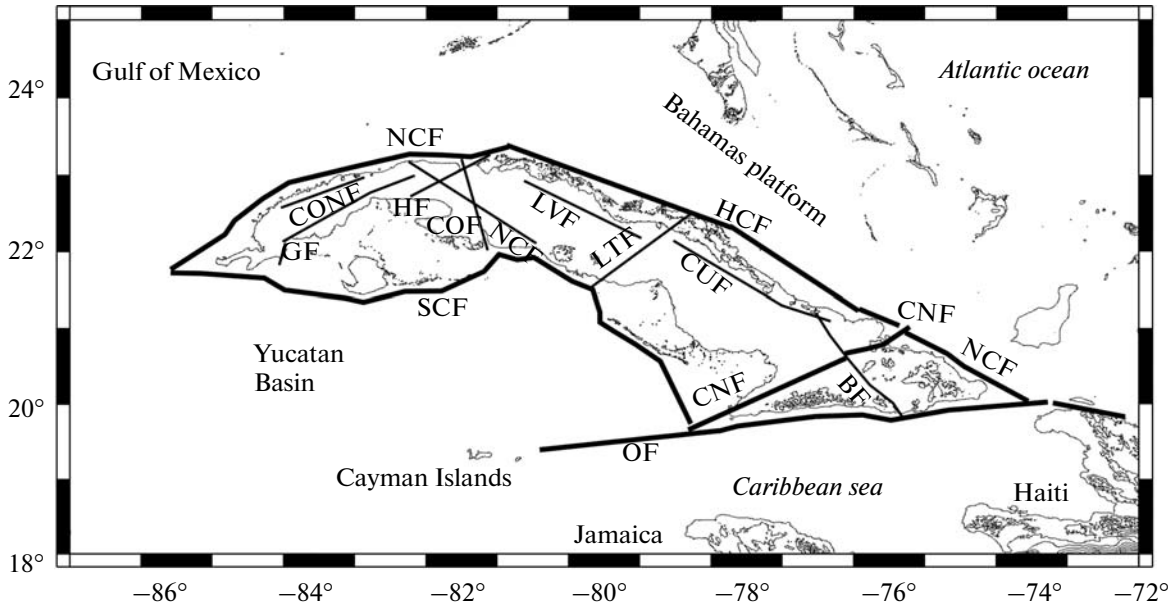

Fig. 4. Active faults of Cuba, according with [24].
BF—Baconao, CNF—Cauto–Nipe, COF—Cochinos, CONF—Consolación del Norte, CUF—Cubitas, GF—Guane, HF—Hicacos, LTF—La Trocha, NCF—Nortecubana, OF—Oriente, SCF—Surcubana.

tonic movements exceeds 1000 m in the Sierra Maestra macroblock. The Cauto river is of the biggest order in the country, with 8 on a scale of 1 : 250000. The continental platform is hardly discernable on the coast.

MATERIALS AND METHODS

The 26 research areas of the Cuban territory studied related to fault zones (Table 1, Fig. 2). Those areas represent approximately 20% of the Cuban surface area. An effort was made to include equal quantitities of all areas. Topographic maps [48–50], aerial panchromatic photographs, scales 1 : 37000 and 1 : 620000 [51, 52], and satellite photographs and imageries (soviet PRIRODA, 1984 (original scale 1 : 1000000); Soyuz, 1975 (original scale 1 : 500000); Landsat, 1975–1978 (channels 5–7)) were all used. A stripe-wise airphoto mosaic set for the different zones was also used in order to trace the drainage network, delineate quaternary sediment areas, and define fracture systems. The works of Cotilla et al. [22] and González et al. [37] supported the results. The information obtained was compared with the results of other specialists [7, 13, 19, 25, 26, 59, 64, 66, 67, 74, 83, 84] and contrasted with the ideas put forward by [24].

On the basis of the photogeological characteristics (i.e., size, shape, tone, texture and drainage pattern) all major geological units were identified following [8, 60]. One type of such geological structures are the lineaments. The term lineament corresponds to all linear elements, generally rectilinear or slightly curvilinear, that intersect topographic surfaces and are connected with geological phenomena that concern bedrock [88]. The identification of lineaments was based on straight river courses, lineaments due to vegetation, differences in topography, and linear contact with different lithologies and soil types evident from the aerial photographs. The interpretation of aerial photographs, satellite imageries and data available from surface mapping clearly illustrates that many oblique to transverse morphotectonic lineaments are oriented across the trend of the island of Cuba.

Field studies have demonstrated that faults are discontinuous geologic features consisting of numerous segments [86]. Even in cross section, fault geometries are quite complex. Individual segments have different lengths and orientations and may transect or truncate adjacent segments. An example is shown in Fig. 4, which contains the Cuban seismoactive fault system according to Cotilla et al. [24]. In particular, we focused on four faults: Cauto–Nipe (CNF), Las Villas (LVF), Nortecubana (NCF), and Oriente (OF). Also, we studied the fractures in nine karstic areas (Baitiquirí, Imías, Yana, La Maqueya, and Punta de Maisí) (Fig. 5) and the joints of three areas (Manicaragua, Cascorro, and Las Cuevas–Potrerillo) (Fig. 6) using also the results of [11, 14, 18–20]. Each locality was approximately 1–5 km in size and each site could cover some tens of metres. The distance between sitesvaried from a few hundred metres to one kilometer. Altogether, 1500 joint orientations were measured at 3 localities. At each locality up to 5 sites were selected, and around 20 measurements were taken at each site. The data were processed using the standard geological method. The fractures were only studied as regards their structure.

Joints are present in rocks in the form of small cracks or fissures. In outcrops they appear at first sight to present a chaotic pattern, but upon closer inspection, distinct systems can be discerned. A first system corresponds to rock layering and the others, to the neotectonic stress–field [72]. Such structures can be inititated during different tectonic events, probably at the same time as when the rock is formed. Nevertheless, most joints were formed during the most recent tectonic movements. Once the orientation of the principal joint systems has been determined, it is possible to locate the orientation of the main stress directions in the neotectonic stress field that caused them [54]. Generally, they are the bisectrices of the other two vertical–subvertical joint systems. The maximum compression axis (P) and the minimum compression axis (T) correspond to the smaller and larger angles, respectively.

In order to evaluate tectonic influence on Cuban river evolution, a brief morphometric analysis of the network was carried out. The Cuban drainage network was first traced on topographic maps and photo mosaic sets using the contour crenulation method (scale 1 : 10000 and 1 : 25000). Finally, it was checked with the use of aerial photographs, Soviet satellite photographs, Landsat satellite images, and field surveys. Every identifiable course of channelled runoff was taken into account and the resulting network was then ordered following the classic method [77]. Finally, the Cuban drainage network was computed to evaluate some important morphometric parameters such as BI (bifurcation index). In addition, the azimuth analysis of drainage networks has become an important tool for identifying the main structural lineaments of a basin area. Moreover, when the study can be carried out within each stream order, a relative temporal reconstruction can also be outlined. In fact, lower order streams of relatively recent emplacement are likely to have been influenced in their development by more recent tectonic movements while higher order streams were influenced by past tectonic movements [32].

To obtain a precise and quantitative azimuth analysis of the streams, the entire channel network was identified by using a digitizer; the digitising process produces a semiautomatic rectification of the network itself. Afterwards, through specific programs in FORTRAN [17], the digitised network was statiscally processed in order to find the most important directions of each stream order (their frequency and standard deviation) as well as the relative length and the total number of segments for each order. To give an indication of how much data was analysed, for the first order more than 2000 streams and 800 rectilinear segments (for a total length of 2030 km) were processed.

In addition to the methods presented in the previous paragraphs to identify and characterize neotectonic movements, Cotilla et al. [27] and González et al. [37] recommend using the following: A) fluvial [27, 28, 32–35, 40, 45–47, 57, 58, 63, 73, 75, 77]: 1) the coefficient of sinuosity (Ks-relationship between the straight-line measurement and the curve measurement of lineal relief elements (rivers, divides, coastlines, etc.) [28]; 2) the significant slope change factor for watersheds and rivers (FC_{cr}); 3) the symmetry/asymmetry index of the fluvial basins along their divides and along their fluvial channels (IS_{cf}/IAS_{cf}); 4) the basin shape and orientation index (IF_{cf}/IO_{cf}) [31]; 5) the visual change factor for the basins (F_{cec}); B) hypsometric-fluvial: 1) the potential intensity of fluvial erosion (IPEF); 2) the elevation/number of intersections of river index (I_{ai}); 3) the river orientation/length index (I_{ol})). All of these parameters can be read as indexes of tectonic influence on channel evolution. In fact, a drainage network characterised by high values for these parameters is likely to be strongly controlled by tectonics [31, 89].

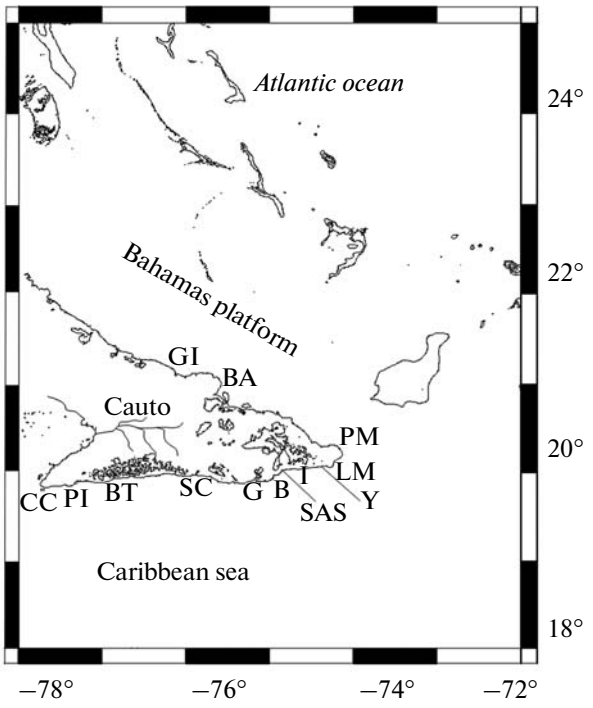

Fig. 5. Eastern Cuba.
Localities: B—Baitiquirí, BA—Banes, BT—Boca del Toro, CC—Cabo Cruz, GI—Gibara, I—Imías, LM—La Maqueyera, PI—Punta del Inglés, PM—Punta de Maisí, SAS—San Antonio del Sur, SC—Santiago de Cuba, Y—Yana.

Related to the analysis of the geological heterogeneous and anisotropic zones (for example, the fractured medium) some very interesting results have been found, such as those put forward by A. Thomas [82]. These are linked to fractal geometry (FG) [56, 62], facilitating the study of irregular, complex phenomena lacking a clearly hierarchical structure at first glance. Consequently, the fractured rock medium and therefore the fracture fields that they constitute, are susceptible to being studied as fractals. The FG offers an alternative model that looks for a quantifiable regular-

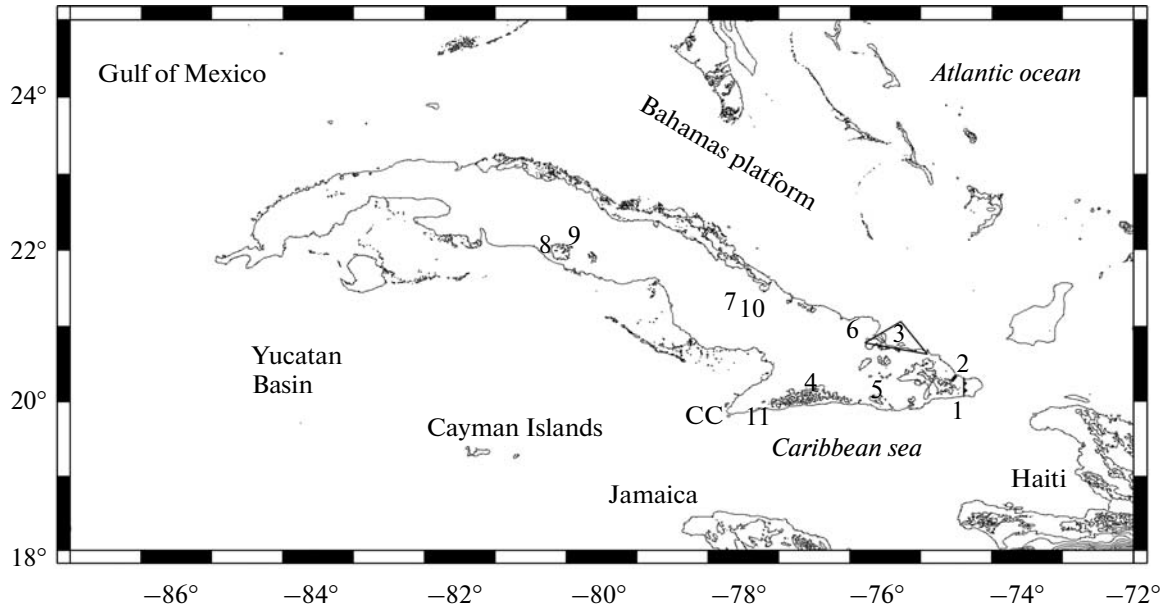

Fig. 6. Study areas of joints.

Localities: 1—morphostructural escarpment, 2—transversal block of Toa–Duaba, 3—downtrow zone of Moa–Nipe, 4—Sierra Maestra Range, 5—Gran Piedra Range, 6—Maniabón, 7—Camagüey, 8—Guamuhaya, 9—Manicaragua, 10—Cascorro, 11—Las Cuevas–Potrerillo, CC—Cabo Cruz.

ity in the relation between an object and its parts, on different scales [61, 62]. In this way repetitive behavior and statistical similarity in the structures, which does not vary with changes in scale, can be appreciated. In addition, the fractal approach to quantifiying fault complexity movement considers two different types of observations of fault geometry and earthquake occurence. Fault trace complexity measured by fractal dimension is also a combination of fault irregularity and fault fragmentation.

One of the physical perceptions which is crucial to a fractal's conceptual definition, is that true structures (such as a fracture itself) evidence statistically similar characteristics on different scales; consequently, they are self-similar. This allows quantifiable information on one scale to be obtained which is of interest to another, given that it obeys hyperbolic type laws or distributions, where the property P is related to the size t through the equation $P \alpha t^{-D}$, D being associated with a fractal dimension. This latter, in generic sense, is a number which serves to quantify the degree of irregularity and fragmentation of a geometric set. The calculation methodology used was based on defining fractures from clusters of points on a line. Given a set of algorithms, it is thus feasible to implement count techniques (box counting), in PC, in order to determine the fractal dimension [61, 87]. R. Bruno, G. Raspa [10], G. Korvin [56], D.L. Turcotte [85] presented sets of models based on the application of several classical techniques. According to D.L. Turcotte [85] the tectonic processes of the earth's crust present an example of deterministic chaos. This is a natural behaviour, implicit in the non-linear equations describing the processes occurring in nature.

The FG was applied to the fractures of two areas (S13, 14, and S15), and to the fluvial network in the area S8–10. For the first two areas the data bases compiled by Barceló et al. [9], Cotilla et al. [26] respectively, were used. In addition, the drainage network of a river was studied using fractal dimension analysis. Even an apparently geometrically irregular trough is characterised by a partial order dependent to various degrees on the structural conditions of the area during the period whilst it was evolving. Following the del Monte et al. [29] method, the fractal dimension D must be evaluated for a significant interval using the formula $D = -\Delta \log N / \Delta \log L$ (where L is the mean length of the streams and N is the number of streams for each interval of given length).

RESULTS AND DISCUSSION

The lineaments map of Cuba (Fig. 7) shows that the majority are straight. These are interpreted as dislocations on a practically vertical plane, or of a dip close to 90°. Lineament distribution is heterogeneous and with different densities depending on their location in the kind of morphostructure. The set of individual alignments was digitized, taking into account the morphostructures in which they appear, in order to carry out a statistical analysis. Next, the lineaments were grouped into azimuth categories for each morphostructure. In this way it was possible to establish that the strike of the majority of lineaments in Cuba

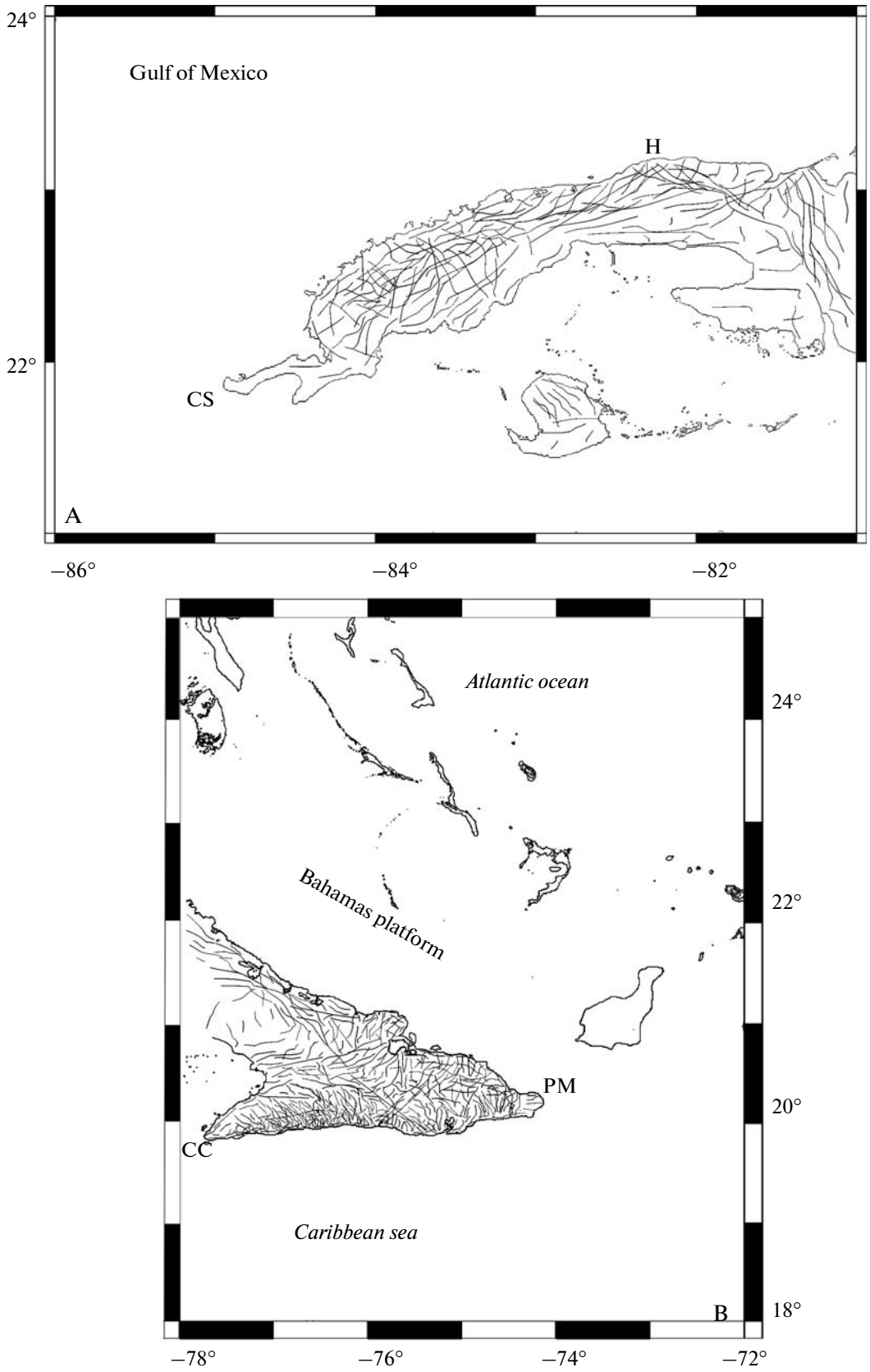

Fig. 7. Lineaments of Western Cuba (A) and Eastern Cuba (B). CS—Cabo de San Antonio, H—La Habana, CC—Cabo Cruz, PM—Punta de Maisí.

Table 2. Characteristics of the morphostructures [39]

No.	Morphostructure	Tendency	Relief type	H_{max}, (m)	Neotectonic Unit	Mesoblocks	Main strike
1	Los Palacios	D	P	110	We	2	NE
2	Batabanó–Manacas–Cienfuegos	D	P	78	We	4	E–W
3	Morón–Redención	D	P	92	We	1	WNW
4	Trocha–Vertientes	D	P	70	We	3	WNW
5	Cauto–Nipe	D	P	70	We	3	WNW
6	Guaniguanico	U	M	699	We	4	NE
7	Habana–Matanzas	U	H	381	We	4	E–W
8	Villa Clara	U	H	443	We	3	NW
9	Guamuhaya	U	M	1156	We	3	E–W
10	Camagüey	U	H	330	We	2	NW
11	Maniabón	U	H	459	We	2	E–W
12	Sierra Maestra	U	M	1974	Ea	2	E–W
13	Guantánamo	U	P	439	Ea	1	NW
14	Nipe–Cristal–Baracoa	U	M	1231	Ea	2	WNW

Note: D—downtrow, U—uplifting, P—plain, H—height, M—mountain, We—western, Ea—eastern

generally varies from E–W, NW, to NE. Several lineaments of NE direction cross different valleys and basins (e.g., the Cauto–Nipe fault). Some of these three groups of lineaments are tear faults and some of the lineaments are also established active faults, identified from ground mapping (e.g., the Baconao fault). In addition, several other lineaments (e.g., Guane) that produce noticeable displacement of rivers and other topographic features are identified as active lineaments.

In Table 1 the characteristics of the 26 research areas are summarized. Meanwhile, Table 2 shows some data for the 14 morphostructures according to González et al. [37]. Two possibilities for each morphostructure were taken in account: 1) number of lineaments, and 2) lineament length. The value for each class is given as a percentage of the corresponding total, both for frequency and for length. All these calculations were carried out automatically using GIS. The results are shown in Table 3. The following should be highlighted: 1) the reduction of linear elements as the chosen length was increased; 2) the persistence of E–W and NW strikes.

Table 4 shows the data on joints from three areas, two from the NUWe (Manicaragua and Cascorro) and one from the NUEa (Las Cuevas–Potrerillo) (Fig. 6). It can be observed that E–W and NW strikes predominate. Results of the fractures study in nine karstic areas (Fig. 5) appear in Tables 5 and 6. It is clearly visible that NNE and N–S strikes predominate in Eastern Cuba, whilst in Southeastern Cuba, E–W strikes predominate. Morover, Table 6 gives information for the Gibara–Banes area, where N–NW, and NE strikes predominate. This latter agrees with the results of Cotilla [11], showing a set of rose-diagrams for the fractures, where S and NW strikes predominate in the emerged and submerged parts. The scheme of fracture density has two areas with maximum value of 5.1 fractures/m^3 for the surroundings of Bariay and Vita bays, and west Gibara (in the Cupeicillo Heights). To facilitate comparison, mean values for fractures per m^3 in selected zones are given: 3.9 in Gibara; 4.6 in Cabo Cruz; 4.4 Punta de Maisí; 3.6 in Cabo de San Antonio; 2.9 in Soroa; and 3.0 in Viñales.

Table 7 shows the location data of eight selected fluvial basins (Fig. 2) from the total identified by Cotilla et al. [22]. Table 8 contains fracture and lineament data regarding quantity and length. The following are of especial note: 1) fracture length in the basins of Santiago de Cuba (1350 km), Toa (862 km), Guantánamo (765 km), Damují (586 km), Canímar (505 km), Mayarí (497 km), Gibara (394 km), and Los Palacios (366 km). It is evident that the maximum value corresponds to Santiago de Cuba, and the minimum corresponds to the NUWe basins. The most important evidence shown in Table 8 is the predominant E–W strike, characterised by high frequency and very low standard deviation. Other recurrent directions shared by almost every order are NW and NE.

Trough morphometric analysis of the drainage network has made it possible to quantitatively verify to what extent tectonics has influenced the evolution of the Cuban megablock network. Moreover, the tectonic lineaments analysed from aerial and satellite photographs, the study of topographic and drainage network anomalies as well as the azimuth analysis of each network segment have highlighted the principal morphotectonic directions of the all studied areas. Tables 9–

Table 3. Statistical analysis of the lineaments (see Table 2)

		Morphostructures														
A		1	2	3	4	5	6	7	8	9	10	11	12	13	14	Σ
	Data	400	685	526	517	728	942	627	716	563	624	576	1.428	1110	1315	10757
	Main strike	NE	E–W	NNW	NW	NNW	NE	E–W	NNW	NW	NNW	E–W	E–W	NNW	E–W	
	Frequency (%)	51.2	49.5	38.7	41.6	38.9	55.6	48.7	53.4	41.5	39.4	55.7	63.8	39.5	41.4	
	Longitude (%)	32.5	40.1	35.7	36.3	29.9	41.2	41.2	48.7	35.4	30.2	49.9	61.2	37.7	40.1	
B	Data	28	200	195	217	433	435	222	270	261	344	281	617	436	547	4486
	Main strike	NNE	E–W	NNW	NNW	NW	NNE	E–W	NW	NW	NW	E–W	E–W	NW	E–W	
	Frequency (%)	48.2	37.7	41.0	38.5	29.8	29.5	41.2	38.7	42.5	41.7	38.9	55.8	47.2	42.3	
	Longitude (%)	40.1	36.0	33.2	37.2	28.8	21.5	33.3	30.1	38.7	36.5	31.3	52.7	40.1	33.2	
C	Data	10	51	47	62	111	157	137	142	58	117	59	188	97	123	1359
	Main strike	NE	E–W	NW	NW	NNW	NE	E–W	NW	NW	NNW	E–W	E–W	NW	E–W	
	Frequency (%)	28.7	42.2	38.8	27.5	28.4	32.5	41.4	39.5	42.4	48.3	35.7	52.3	47.8	39.0	
	Longitude (%)	25.0	32.1	30.2	25.5	26.1	30.0	37.3	31.5	29.8	37.9	28.2	42.0	38.6	31.2	
D	Data	5	17	21	22	45	47	45	48	12	40	21	87	31	38	479
	Main strike	NE	E–W	NW	NW	NW	NE	E–W	NNW	NW	NW	E–W	E–W	NNW	E–W	
	Frequency (%)	50	31.88	28.92	42.71	38.95	42.33	39.42	40.01	37.72	31.67	45.27	52.25	46.72	54.83	
	Longitude (%)	47.16	29.58	21.85	39.47	35.16	37.88	35.23	36.85	30.81	28.47	38.16	47.29	41.85	49.77	

Note: A—all lineaments, B—lineaments with L > 2 km, C—lineaments with L > 5 km, D—lineaments with L > 10 km.

Table 4. Joints of three areas

	Quantity by zone											
	Manicaragua				Cascorro					Las Cuevas–Potrerillo		
	1	2	3	Σ	4	5	6	7	∑	8	9	Σ
10–20°	28	32	37	97	19	19	22	16	76	10	10	20
40–50°	25	19	19	63	40	41	35	27	143	17	10	27
50–60°	28	26	30	84	19	25	19	10	73	10	7	17
80–90°	26	28	31	85	10	15	8	12	45	5	3	8
100–110°	15	15	12	42	17	17	25	16	75	5	2	7
140–150°	5	10	10	25	20	15	14	15	64	29	35	64
160–170°	10	12	10	32	22	27	20	28	97	22	16	38
170–180°	47	36	45	128	25	24	28	28	105	48	55	103
Σ	184	178	194	556	172	183	171	152	678	146	138	284

Note: Area 1—Upper Cretaceous plagiogranite and doarites (Manicaragua, Guamuhaya Mountain); Area 2—Upper Cretaceous granite and plagiogranite (Cascorro, Gamagüey); Area 3—Middle Eocene (granite (Las Cuevas—Potrerillo, Sierra Maestra Mountains)

Table 5. Fractures of the Eastern and Southeastern Cuba

	Eastern Cuba						Southeastern Cuba			
	1	2	3	4	5	Σ	6	7	8	Σ
10–20°	–	–	–	–	80	80	–	–	–	–
40–50°	–	–	–	–	–	–	10	16	16	42
50–60°	78	88	85	90	–	341	–	–	–	–
80–90°	90	98	87	100	8	383	–	29	70	99
100–110°	85	90	78	90	58	401	22	17	16	55
140–150°	67	70	50	56	–	243	78	5	22	105
170–180°	10	7	6	1	85	109	28	47	85	160
Σ	330	353	306	337	231	1557	138	114	209	461

Note: 1—Baitiquirí (Q); 2—Imías (N_2–Q); 3—Yana (Q); 4—La Maqueyera (Q_{II}–Q_{III}); 5—Punta de Maisí (Q_{II}–Q_{III}); 6—Cabo Cruz (Q_{II}–Q_{III}); 7—Punta del Inglés (Q_{II}–Q_{III}); 8—Boca del Toro (Q_{II}–Q_{III}).

14 contain all data obtained for the 26 rivers and basins selected. The river of the biggest order (8) is the Cauto, and the largest quantity of fluvial currents is of the order five. There are three rivers with markedly anomalous coefficient of sinuosity (S4 (Negro–Hanaguanico), N4 (Almendares), N6 (Canímar)), all in the NUWe. This result corresponds to index values for Gavelius and Rugosity. The rivers witfi the largest quantity of anomalous sectors are S8 (Cauto) and N3 (Toa), both in the NUEa.

It is notable that the Bayate river (Fig. 8), at the N1–N3 sector to the east ofthe locality of San Cristóbal does not have fluvial inflections. However, the rivers to the west of San Cristobal (Bacunagua, Los Palacios, San Diego, Herradura, Hondo, Ajíconal, Feo Guamá, San Juan y Martínez, and Cuyaguateje) have some inflections, permiting the identification of an SW–NE alignment on the south plain of Pinar del Río, corresponding to the Guane fault, whith was responsible for the San Cristóbal earthquake on the 28.01.1880 (I = 8 MSK) [12].

The Sierra Maestra range (h ~ 2000 m) has a very acute transverse differentiation which is related to its vicinity to the structure of the Oriente trough (h ~ –8000 m) [38]. In the southern part of the Sierra Maestra, with a N–S profile, the rivers have on the average a length of 15 km and a width of 5 km. A correlation graph of these rivers (Fig. 9) displays their geometric and morphometric characteristics. In contrast, in the northern part, characteristic river measurements are 60 km in length and 15 km wide. The south side of the Sierra Maestra is transversely intersected by a group of fluvial currents with a mean slope of 35–40° and significant deformations in their basins and principal valleys. The majority of the transverse spectra of the fluvial terraces are affected by asymmetric faults. In relation to this,

Hernández et al. [43] give the following data for the Carpintero river, located between Santiago of Cuba bay and Baconao; basin area 17.3 km^2; maximum height of the river 1000 m, length of the principal river 8.9 km, mean slope of the main river 49.0‰. This coincides with our results for the Sardinero and San Juan rivers, also in the same sector, which have six anomalous sectors.

There are three parallel rivers with a NW strike, and issuing in the north part of the Sierra Maestra range (Bayamo, Cautillo, and Contramaestre) which drain into the south side of the Cauto river. In contrast, in that same segment, but on the north side of the Cauto river, there is only one river course (the Salado river) with a fluvial course approximately parallel to the Cauto river. The affluents of the Salado river only run from the north side in southwest strike. This coincides with the results found by G. García [36] who states that the lineament pattern in the Cauto zone is formed by two systems: 1) one conjugated, N30°, E40°–N330°, W315°, 2) N50°, E60°. The Cauto has 14 fluvial terraces according to Hernández et al. [42], however, the authors have identified only 10. The affluents ofthe Cauto river (Contramaestre, Bayamo, Cautillo and Yara), according to Hernandez et al. [42], have 13 terraces whereas we identified 10. Our results coincided with those authors only with respect to the Salado river, which has five terraces. That is to say, we would claim that the trend of the river cut is important, but less so than that claimed by other authors. The Cauto–Nipe fault (150 km), with a NE strike, is linked to this zone, and was responsible for the following earthquakes: 18.10.1551 (I = 8 MSK), 19.07.1962 (I = 6 MSK), 11.04.1987 (I = 4.5 MSK), 27.03.1988 (I = 4 MSK), 29.03.1988 (I = 4 MSK), 19.07.1962 (I = 6 MSK).

Throughout the southeastern coast of Cuba there are several quaternary tectonic troughs, among them: Cajobabo, Imías, San Antonio del Sur, and two bays (Santiago de Cuba and Guantánamo) with strong tectonic influence. The geometric shape of those two bays, the most important ones in the southeastern region, are differentiated as regards lithology, morphology, and the densities and direction of the fractures. In Santiago de Cuba the prevailing strike is from NE to NNE and in Guantánamo, N–S and E–W. In contrast, the Pilón bay and the Baconao lagoon are depressed tectonic structures, graben style with an elipsoidal morphology, showing their greatest axis in an approximate E–W strike. They are in the Western and Eastern morphostructures, respectively, of the Sierra Maestra, and in contraposition with the deepest extremes of the Oriente trough. These observations can be considered as morphographic characteristics of the Oriente fault. From the west of Baconao to the Punta de Maisí, the emerged relief of the Oriente fault is totally different from the previous sector, emphasizing the gentle profile of the Sabana la Mar river in San Antonio del Sur. Basin asymmetry index is 1/10. The fluvial network in this sector mainly flows parallel to the southern coast line. Given the undisputed morphology of active tectonics in the south of Eastern Cuba, Cotilla et al. [25] proposed a system of scissor faults for a segment of the southern Sierra Maestra range (Fig. 10). This model explains adequately the presence of the Sierra Maestra and the South Guantánamo marine terrace systems (Fig. 11), as well as the Boniato and Baconao faults in north.

For the most eastern part of Cuba (approximately in the 74°30′ W) the rivers to the east of the already

Table 6. Fractures in Gibara–Banes karstic area

	Quantity		Longitude, km	
	F	L	F	L
0–10°	46	99	50	95
10–20°	31	10	45	66
20–30°	25	92	28	45
30–40°	26	85	20	41
40–50°	33	101	46	72
50–60°	28	100	39	50
60–70°	10	66	17	26
70–80°	11	50	19	31
80–90°	63	168	95	130
90–100°	39	140	73	102
100–110°	31	102	39	48
110–120°	9	63	15	29
120–130°	26	80	12	26
130–140°	14	54	18	26
140–150°	12	50	20	44
150–160°	25	105	40	66
160–170°	27	110	43	68
170–180°	11	67	20	43
Σ	467	1.642	639	1008

Note: F—fracture, L—lineament

Table 7. Basins data

No.	Basin	Coast	Neotectonic Unit
1	Santiago de Cuba	South	Eastern
2	Guantánamo	South	Eastern
3	Gibara	North	Western
4	Los Palacios	South	Western
5	Damují	South	Western
6	Toa	North	Eastern
7	Mayarí	North	Eastern
8	Canímar	North	Western

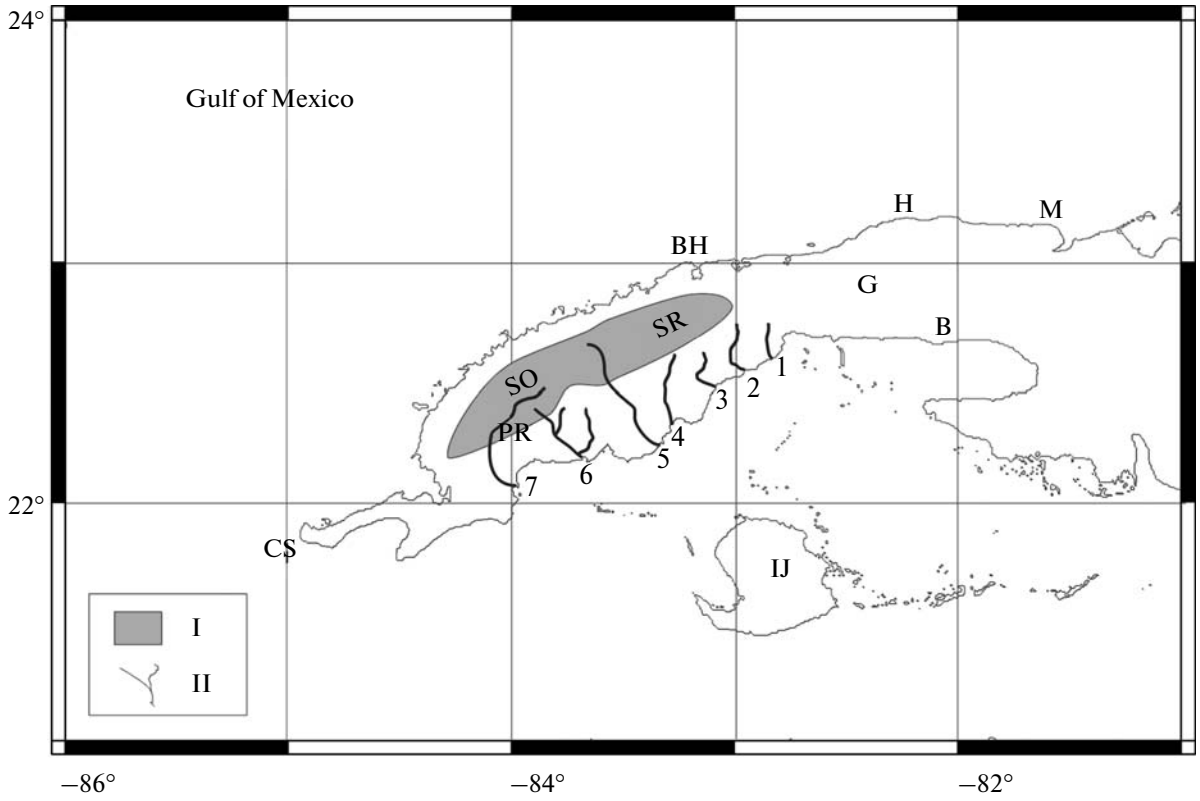

Fig. 8. Rivers of southwestern Cuba.
I—shadow area—Guaniguanico Mountains: SO—Sierra de los Órganos, SR—Sierra del Rosario; II—rivers: 1—Bayate, 2—San Cristóbal, 3—Bacunagua, 4—San Diego, 5—Hondo, 6—Feo–Agabama, 7—Cuyaguateje. Localities: B—Batabanó, BH—Bahía Honda, CS—Cabo de San Antonio, G—Guanajay, H—La Habana, IJ—Isla de la Juventud, M—Matanzas, PR—Pinar del Rio.

mentioned Sabana la Mar river drain approximately perpendicularly to the southern coast line. This is also the case for the rivers (Baracoa and Yumurí) that drain into the northern coast, on the same geographical longitud. A morphostructural step falling to the east for a meridian between Punta Caleta (south coast) and Punta Silencio (north coast) (Fig. 6) has been mapped for the first time via field work. In that sector it drains to the east of the Maya river (of 3rd order) from Gran Tierra toward Punta de Maisí with a Ks = 0.95 and with mean slope of 48.5‰.

The fluvial density to the east of Moa to Punta Garito has much higher values, and the rivers (Yagumaje, Cayo Guam, Quesigua, and Jiguani) show a more defined canyon formation than those located to the west. Specifically, to the west, the coast is submerged until the Nipe bay (this includes the section Moa–Sagua to Tánamo–Mayari–Bahía to Nipe). Also to the west, but 74°40′ W of the north coast, all the rivers drain approximately perpendicularly to the coast until the Nipe bay, where the mouth of Mayarí river is located. However, the Toa and Duaba rivers run parallel toward the north coast, west of Baracoa, for some 20 km with a separation of 10 km. This regularity has also been observed to a lesser extent for all the rivers in the coastal segment to the west of the Toa to Punta Guanico, exactly north of the meridian of San Antonio del Sur. Therefore, these elements could be indicative of a new tectonic influence, given that they break with the regularity of the ancient structures.

With regard to the Moa region, Rodríguez et al. [70] stated that the principal limits of the six blocks they identified are the active faults: Los Indios, Miraflores, Cabaña, Moa, Cayo Guam, and Quesigua. Furthermore they claim that the Quesigua fault is responsible for two recent earthquakes; that all those faults are displaced 1.5 km in some sites by a strike-slip fault of NW–SE strike, designated Sabana; and that the youngest system has a north strike, but that this is not evident in the relief due to its youth. Later, Rodríguez et al. [69] stated that the Quesigua fault was responsible for some earthquakes in 1992. They also claimed that this fault, 7.5 km length in N–S direction, is cut by another, younger, fault, called El Medio. In addition, A. Rodríguez, J. Blanco [68] asserted that El Medio and Cananova faults (also in Moa) cut and displaced each other. Evidently, all these data and conclusions are erronous because an active fault of such dimensions, and displaced by other similar structures, can not be responsible for an earthquake. Cotilla et al.

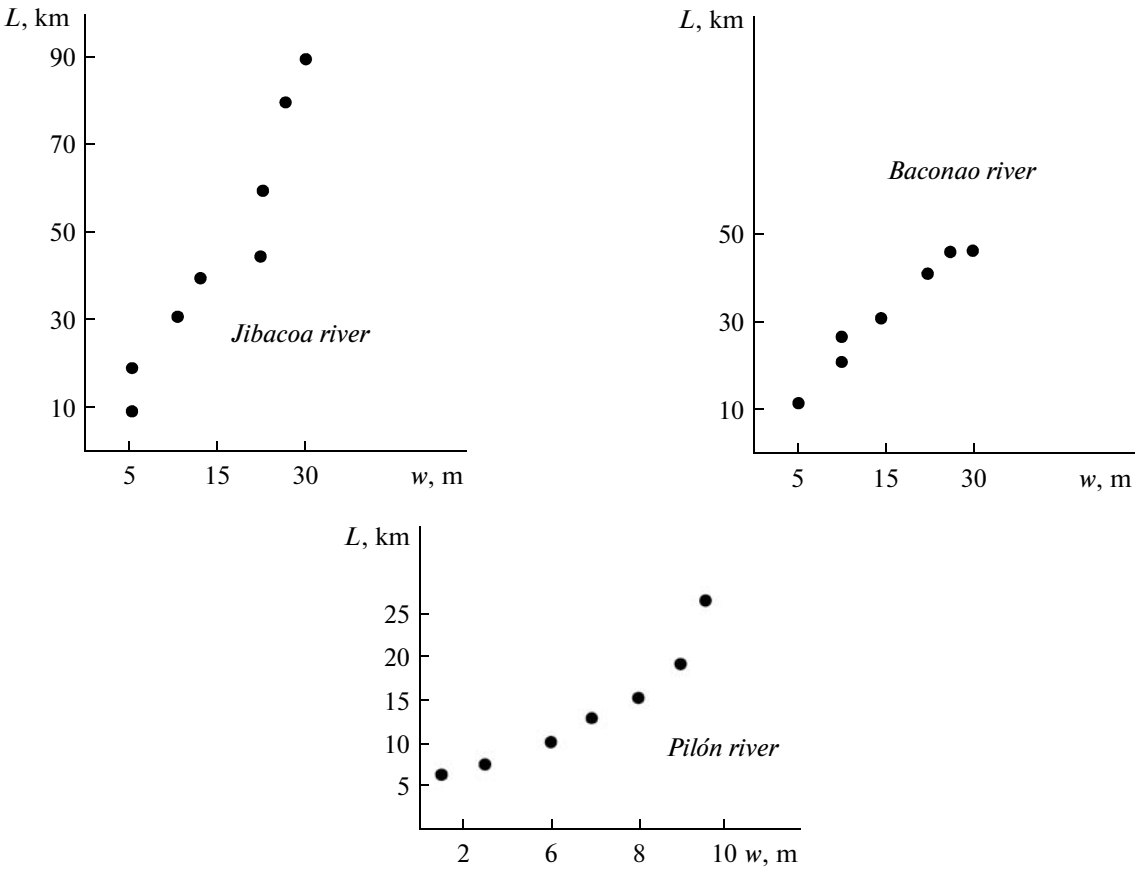

Fig. 9. Statistical correlation (longitude—wide) of the three rivers (Jibacoa, Baconao, Pilón) in the Sierra Maestra.

[24] discussed this series of earthquakes in 1992 in the Moa region, and pointed out that the seismogenic Norte Cubana fault was responsible, as previous stated Cotilla [12].

It can be asserted that the fracture strikes identified by aerial photographs, and the strikes of the straight stretches of the fluvial network in the morphostructural zone bear, in general, a close relation, as regards the Santiago de Cuba and Guantánamo bays. The graphic correlation demonstrates a reliable level of adjustment with acceptable deviation (Fig. 12).

It has been confirmed that a set of characteristic neotectonics exists in southeastern Cuba which facilitates the differentiation, in at least two parts or segments (Western: Cabo Cruz—Santiago de Cuba; Eastern: Santiago de Cuba—Punta de Maisí), from the Oriente fault as follows: 1) the Ks = 0.96 of the second branch of the main watershed, in the western section (on the Sierra Maestra); 2) the parallelism and proximity, of the branch of that watershed on the Sierra Maestra, to the southeastern coast; 3) the spatial contraposition of the Sierra Maestra and the Oriente trough, with an approximate drop of 10 km in a section with 20 km of separation; 4) the prevailing N–S strike, the reduced superficial dimension and the rectangular shape of the river basins to the south of the Sierra Maestra; 5) the greater slope (48%) of the rivers; 6) the greater altimetric levels (1974 m); 7) the greater extent of the uplifting neotectonic movements (1790 m); 8) the greater number of marine terraces (predominance on 5 levels) in the south of the Sierra Maestra; 9) the greater number of anomalous sectors of river; 10) the greater quantity of deformations in the marine terraces; 11) the steeper profile and the systems of the closest terraces; 12) the transverse asymmetry of the Pilón and Baconao basins in the western and eastern extremes of the Oriente trough; 13) the diferentiation with respect to fracturing in the two most important bays (Santiago de Cuba (2865) and Guantánamo (1372)). This shows a high level of agreement with the seismic activity and epicentre density maps [12]. Also the maximum registered magnitude of earthquakes and estimates based on historical data is greater in the western segment that in the eastern, taking the zone of Baconao as a reference [12].

In Eastern Cuba there are four faults that determine its seismic activity. These are the Oriente, Nortecubana (NCF), Cauto–Nipe (CNF) and Baconao faults. Thus, the western and eastern extremes of Eastern Cuba, Cabo Cruz and Punta de Maisí, respectively, can be used to establish the links in this segment between the Oriente fault and the associ-

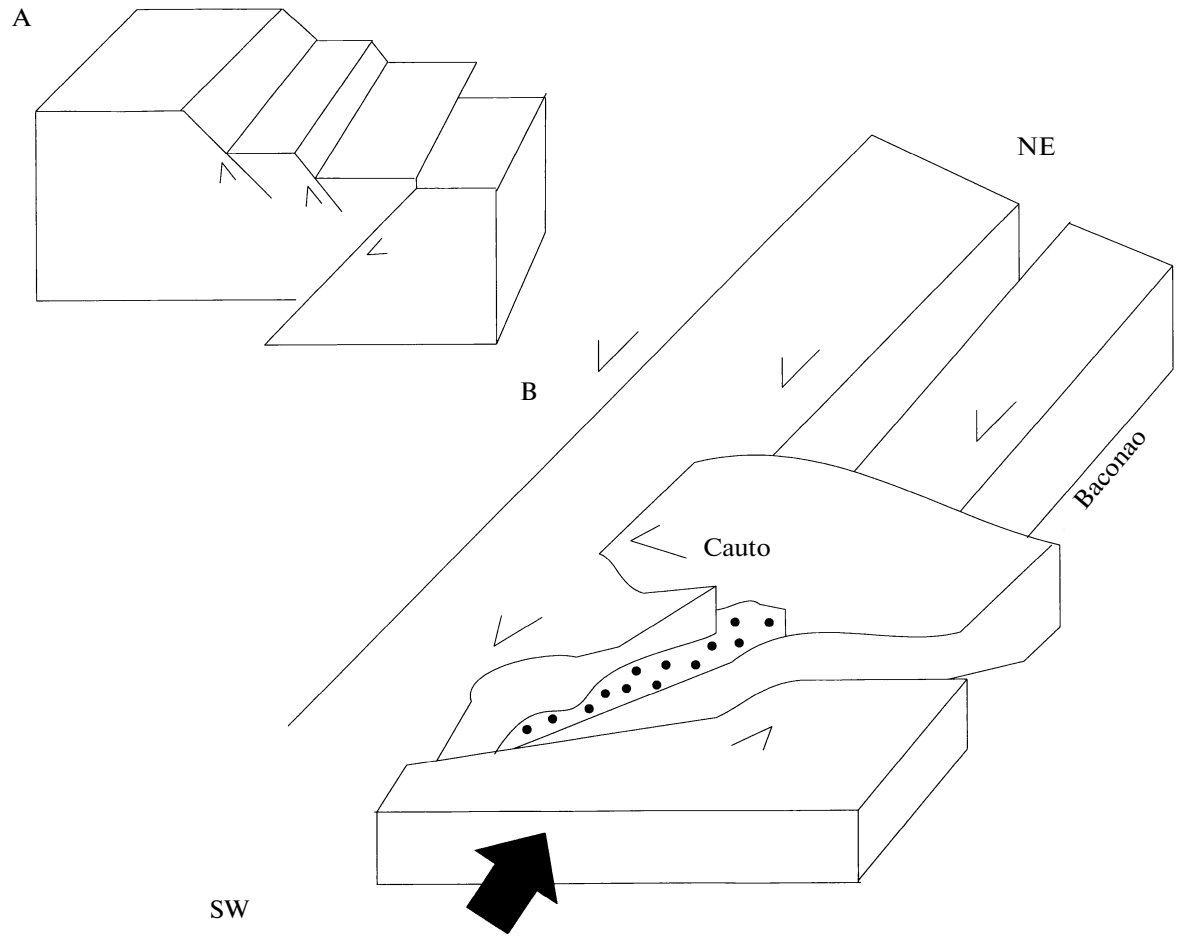

Fig. 10. Models of fault systems in Southeastern Cuba: A—Sierra Maestra–Oriente trough zone, B—Cauto–Nipe zone.

ated faults of Cauto–Nipe with NE–SW strike and Nortecubana with NW–SE strike. At both extremes there are seismic events, the strongest in Cabo Cruz (26.08.1990, M_s = 5.9; 25.05.1992, M_s = 6.9; 04.02.2007, M_w = 6.2). The associated faults mentioned above, have a different kinematic CNF (left strike-slip) and NCF (compressive). Cauto–Nipe area constitutes a continental pull–apart basin, while the NCF represents a longitudinal marine depression. Cotilla et al. [23] state that CNF has two very well differentiated segments following the intersection with the Baconao fault (240 km), in the area around San Germán. In this way they are joined at their south and north extremes, through the formation of knots, with the OF and NCF, respectively. In both knots there are earthquakes, but the southern knot, Cabo Cruz, is the most active of the three. Paradoxically, in spite of the fact that this fault is surrounded by permanent seismic stations, it has not been studied, due to administrative decisions [12].

The fault NCF is a large submarine structure (>1000 km) which has been identified as the northern boundary of the Cuban megablock [23]. It has three segments: Western (from Cabo de San Antonio to the Peninsula de Hicacos), Central (from Peninsula de Hicacos to Cauto–Nipe), and Eastern (from Cauto–Nipe to the Punta de Maisí). Each section is associated with seismic events during instrumental and historical periods (Central: 28.02.1914, Gibara (M_s = 6.2); 15.08.1939, Remedios–Caibarién (M_s = 5.9); 25.05.1960 (I = 5 MSK); 18.12.1986 (I = 4 MSK); Eastern: 05.01.1990 (mb = 4.5), 20.03.1992 (M_s = 4.0), 24.09.1992 (I = 5 MSK), 28.12.1998 (mb = 5.4)). Cotilla [12] questioned, with scientific arguments, the differentiation of the eastern and central segments, and the operational subjectivity of the Cuban seismic station network during the period 1980–1990, which hindered accurate measurement of the eastern segment's seismic potential. This author also suggested that both segments could be differentiated according to the influence of tensile force and the faults' movement mechanisms, from their location and disposition with respect to the Bahamas Platform. Furthermore, westward of Cauto–Nipe the OF fault is connected with the Cayman sea floor spreading centre, already mentioned. In this part there are strong seismic events

A

B

C

Fig. 11. Marine terraces of Southeastern Cuba (Sierra Maestra Range): A—Pilón, B—Santiago de Cuba, C—Baconao.

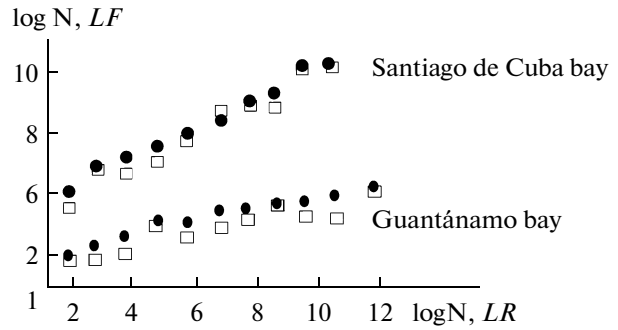

Fig. 12. Statistical correlation (fractures—strikes) of Santiago de Cuba and Guantánamo bays.

(07.07.1852; I = 9 MSK; M_s = 7.5; Virgin Islands), whilst to the east of the Punta de Maisí the fault extends to northern Haiti and then enters the Dominican Republic, as the North fault. The strongest plate boundary zone earthquakes occurr at these sites.

From Cabo de San Antonio to the Punta de Maisí (west–east) the profile of the NCF fault changes strike and configuration in the Peninsula de Hicacos, from NE to NW. The western segment adjoins an oceanic structure (the Gulf of Mexico) to the north, the central segment is adjacent to the widest part of the Bahamas Platform, and the eastern segment is adjacent to the Bahamas Platform and the Atlantic Ocean. The strongest seismic activity of the NCF fault, with respect to maximum earthquake magnitude, is located in the central segment (15.08.1939, M_s = 5.9 in the Carribean; 28.02.1914, M_s = 6.2 in Gibara).

The faults of the northern continental part of Cuba are spatially analogous to the NCF fault strike. Thus, the Pinar del Río and Guane faults (NUWe) have NE strikes and are parallel to the western segment of the NCF, whilst the Las Villas and Cubitas faults, also in the same NUWe, are parallel to the central segment of the NCF. They are all seismically active. However, in the continental part of the NUEa there is not a single fault displaying this regularity in comparison with the eastern segment of the NCF. Therefore, the insular faulting structures have inherited the strike of the system's main fault, the NCF, except in the final section. The seismicity of the eastern segment is greater than that of western, but much less than the central. It should also be emphasized that in the zone of strike change from NE to NW for the NCF fault, in Punta de Hicacos, there is a set of faults in the Cuban insular part whose cartography corresponds to this situation. They are Habana–Cienfuegos, Cochinos and Hicacos.

As for the Baconao fault, this is shown by the combination of the Baconao River which drains to the SE on the southeast coast, and the Guananicum River, which drains into the Cauto on a NW strike. This fault is associated with the following earthquakes: 05.03.1927 (I = 7 MSK), 13.05.1951 (I = 6 MSK), 06.06.1990 (I = 4 MSK), and 03.10.1990 (I = 4 MSK).

The neotectonic investigations carried out by Cotilla et al. [23] permitted, for the first time, the diferentiation of three segments of the Oriente fault. It is a submarine structure and therefore, regrettably, it is not possible to apply the fractal methodology developed by P.G. Okubo, K. Aki [65] for the study of the San Andrés fault. However, for this research an alternative has been used to quantify the differentiation of the

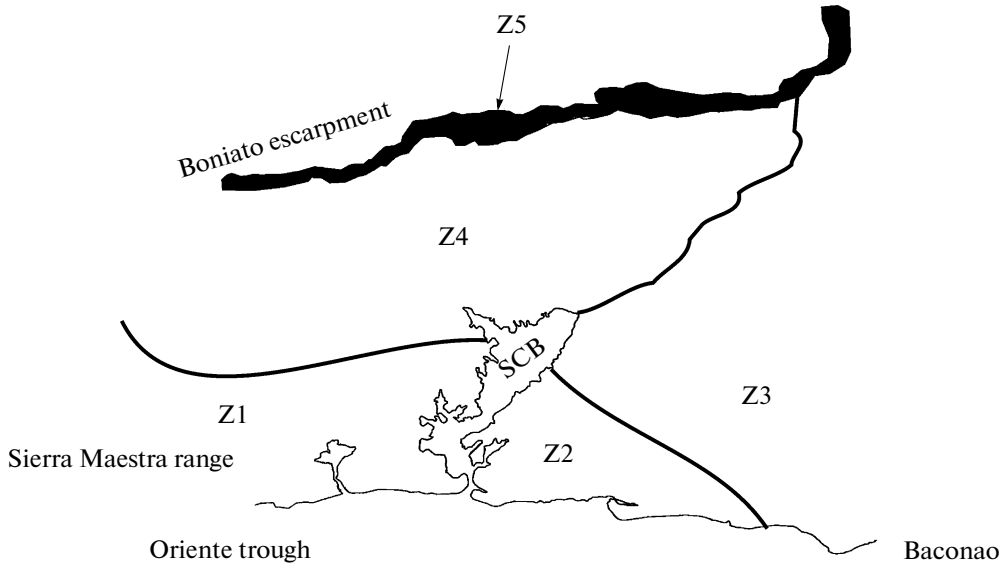

Fig. 13. Morphostructural zones (5) in Santiago de Cuba bay. SCB—Santiago de Cuba bay, Z—Zone.

Table 8. Fractures in fluvial basins (see Table 7)

	Santiago de Cuba				Guantánamo				Gibara				Los Palacios			
	Quantity		Longitude, km		Quantity		Longitude, km		Quantity		Longitude, km		Quantity		Longitude, km	
	F	L	F	L	F	L	F	L	F	L	F	L	F	L	F	L
0–10°	10	28	24	37	28	47	49	65	11	18	17	23	5	11	7	10
10–20°	15	29	28	44	28	41	43	55	13	25	20	31	3	7	7	12
20–30°	19	31	27	54	19	29	37	44	11	17	14	28	5	15	10	17
30–40°	19	36	29	55	5	10	12	25	21	26	29	35	7	15	11	17
40–50°	45	65	54	89	9	12	16	23	9	13	12	21	11	22	18	24
50–60°	98	110	120	138	10	22	29	38	5	11	10	19	18	27	23	33
60–70°	110	150	116	165	22	34	38	50	12	21	17	25	26	33	33	37
70–80°	100	180	101	276	55	78	66	98	24	23	36	45	26	37	36	44
80–90°	150	160	198	219	57	90	70	119	13	28	27	33	31	41	41	51
90–100°	155	120	156	188	51	88	48	100	22	33	35	44	41	55	50	61
100–110°	120	160	160	238	39	76	47	101	10	25	24	32	16	28	25	33
110–120°	76	80	89	111	40	54	54	76	15	29	21	31	12	17	24	39
120–130°	46	58	60	87	15	20	39	50	7	15	16	28	10	15	17	25
130–140°	19	29	39	66	10	12	27	48	10	21	15	30	11	16	19	30
140–150°	29	39	40	68	19	29	29	58	10	19	14	19	13	21	20	23
150–160°	25	30	48	75	36	45	48	68	20	31	29	41	5	10	9	15
160–170°	19	20	33	45	44	56	56	77	16	30	21	35	4	7	9	17
170–180°	10	25	28	44	48	60	57	89	25	42	37	51	3	5	7	13
Σ	1046	1350	1350	1999	535	803	765	1184	254	437	394	571	247	382	366	500

Table 8. (Contd.)

	Damují				Toa				Mayarí				Canímar			
	Quantity		Longitude, km		Quantity		Longitude, km		Quantity		Longitude, km		Quantity		Longitude, km	
	F	L	F	L	F	L	F	L	F	L	F	L	F	L	F	L
0–10°	17	27	22	34	40	55	47	59	16	28	20	31	10	19	17	28
10–20°	12	24	20	29	35	48	46	59	10	25	22	33	15	24	23	41
20–30°	13	24	19	26	19	31	25	31	10	27	21	31	11	22	19	30
30–40°	25	31	33	39	28	40	36	47	30	41	43	55	27	33	41	62
40–50°	30	39	38	42	30	37	41	50	5	11	11	19	20	29	28	39
50–60°	36	42	47	55	17	29	22	37	4	7	9	15	17	28	25	39
60–70°	41	47	45	52	15	28	24	29	12	27	25	41	28	41	41	55
70–80°	40	46	47	51	36	45	48	60	27	41	41	60	39	50	47	54
80–90°	45	55	55	62	38	52	51	63	18	33	33	55	41	61	48	67
90–100°	39	45	49	57	42	50	55	68	30	42	43	49	41	63	52	65
100–110°	40	48	51	61	47	55	61	77	17	28	28	41	19	29	27	33
110–120°	23	36	40	51	19	29	30	45	3	10	10	21	28	40	36	48
120–130°	19	27	28	34	29	37	37	49	11	25	27	33	11	22	25	41
130–140°	19	29	27	33	41	51	51	63	9	24	15	23	7	14	15	37
140–150°	17	26	21	32	39	51	55	69	17	30	27	41	10	21	19	39
150–160°	12	19	17	28	51	66	70	88	17	35	32	55	15	33	23	41
160–170°	10	17	16	29	61	77	79	92	22	31	40	54	4	11	8	16
170–180°	5	9	11	15	62	80	84	116	31	50	50	65	5	10	11	27
Σ	443	591	586	730	649	861	862	1102	289	515	497	722	348	550	505	762

Note: F—fracture, L—lineament.

Table 9. Data of the rivers by basin

River		Maximum order						Bifurcation relation							Sinuosity coefficient by		Indexes		Longitude, km
Acronym	Denomination	3	4	5	6	7	8	1–2	2–3	3–4	4–5	5–6	6–7	7–8	Longitude	Altitude	Ig	Ir (×100)	
S1	San Cristóbal	–		X	–	–	–	4.9	4.4	4.8	4.3	–	–	–	0.80	0.75	0.75	1.61	62
S2	Bacunagua	–	–	X	–	–	–	5.0	4.5	4.3	4.3	–	–	–	0.81	0.78	0.76	1.60	60
S3	San Diego	–	–	X	–	–	–	5.0	4.4	4.7	4.1	–	–	–	0.83	0.78	0.75	1.59	86
S4	Negro–Hanaguanico	–	X	–	–	–	–	4.8	2.0	2.0	–	–	–	–	0.50	0.49	0.46	0.81	55
S5	Damují	–	–	X	–	–	–	5.0	3.5	3.1	2.0	–	–	–	0.70	0.65	0.82	1.60	62
S6	Zaza	–	–	–	X	–	–	4.8	4.7	3.6	3.3	2.5	–	–	0.68	0.60	0.71	1.57	145
S7	Agabama	–	–	–	X	–	–	4.9	5.0	5.0	4.6	2.7	–	–	0.90	0.81	0.70	1.59	118
S8	Cauto	–	–	–	–	–	X	5.0	5.1	5.0	4.6	3.7	3.8	4.0	0.95	0.93	0.82	1.76	343
S9	Limones	X	–	–	–	–	–	3.0	5.0	–	–	–	–	–	0.72	0.67	0.61	1.61	42
S10	Jibacoa	–	–	–	X	–	–	5.0	4.5	4.6	4.7	3.8	–	–	0.80	0.68	0.76	1.70	90
S11	Pilón	X	–	–	–	–	–	4.8	4.8	–	–	–	–	–	0.98	0.95	0.71	1.62	28
S12	Maya	X	–	–	–	–	–	3.9	4.2	–	–	–	–	–	0.80	0.79	0.58	1.55	35
S13	San Juan	–	X	–	–	–	–	3.9	3.0	–	–	–	–	–	0.81	0.79	0.62	1.59	30
S14	Sardinero	X	–	–	–	–	–	4.0	3.0	3.0	–	–	–	–	0.80	0.79	0.60	1.58	31
S15	Bacoano	–	X	–	–	–	–	4.0	3.6	3.0	–	–	–	–	0.77	0.71	0.61	1.50	54
S16	Guantánamo	–	–	–	X	–	–	4.4	4.0	5.0	3.6	3.0	–	–	0.78	0.70	0.73	1.70	98
S17	Sabana la Mar	–	–	X	–	–	–	4.3	4.2	3.9	3.0	–	–	–	0.80	0.76	0.70	1.70	55
N1	Mayarí	–	–	–	–	X	–	4.8	4.5	4.1	3.2	3.1	2.5	–	0.92	0.89	0.70	1.70	107
N2	Moa	–	–	X	–	–	–	4.9	4.7	4.6	3.7	–	–	–	0.82	0.79	0.71	1.69	45
N3	Toa	–	–	–	–	X	–	4.8	4.8	4.1	3.9	4.0	3.2	–	0.76	0.72	0.81	1.79	118
N4	Almendares	–	–	X	–	–	–	5.0	5.0	4.6	4.6	–	–	–	0.45	0.42	0.38	0.82	50
N5	Jaruco	–	–	X	–	–	–	4.3	4.4	4.6	4.6	–	–	–	0.72	0.70	0.87	1.80	31
N6	Canímar	–	X	–	–	–	–	2.4	4.6	2.0	–	–	–	–	0.51	0.49	0.48	0.72	50
N7	Sagua la Chica	–	–	–	X	–	–	4.4	4.9	3.4	3.3	3.0	–	–	0.72	0.71	0.60	1.56	91
N8	Jatibónico del Norte	–	X	–	–	–	–	3.3	3.5	2.0	–	–	–	–	0.72	0.72	0.61	1.58	70
N9	Gibara	–	–	X	–	–	–	5.0	4.5	4.5	4.0	–	–	–	0.87	0.85	0.70	1.65	64
Total = 26		4	5	9	5	2	1												2030

Note: Ig—Gavelius Index, Ir—Rugosity Index.

Table 10. Predominant strike of the rivers and basins/anomalous river sectors (see Table 9)

River	Order								Strike	
	1	2	3	4	5	6	7	8	Main river	Basin
S1	S/5	S/5	S/2	SE/1	SE	–	–	–	SE	SE
S2	S/3	S/3	SE/1	S	S	–	–	–	S	SE
S3	S/4	S/2	SE/1	S	S	–	–	–	S	S
S4	W	S/1	SW/1	W	–	–	–	–	W	SW
S5	SE/2	S/1	SE	SE	SE	–	–	–	SE	S
S6	SE/8	S/3	SE/3	SW/1	SW	SW	–	–	SW	S
S7	S/9	S/4	SE/4	SE/2	S	S	–	–	S	S
S8	N/85	NW/89	NW/40	NW/15	NW/10	NW/4	NW/6	W/2	W	E–W
S9	NW/2	W/2	W	–	–	–	–	–	W	E–W
S10	NW/5	NW/5	NW/2	NW/2	NW/1	WNW/1	–	–	WNW	NW
S11	S/5	S/5	S/1	–	–	–	–	–	SE	S
S12	NE/1	E/2	E	–	–	–	–	–	E	W–E
S13	S/5	S/2	S/1	–	–	–	–	–	S	S
S14	S/3	S/2	S/1	S/1	–	–	–	–	S	S
S15	S/10	SE/4	SE/1	SE/1	–	–	–	–	SE	SE
S16	S/10	S/5	SE/2	SE/2	S/1	S	–	–	S	SE
S17	S/16	S/7	SW/2	SW/1	SSW/1	–	–	–	SSW	SSW
N1	N/25	N/18	NNE/5	N/5	NE/2	N/2	N/1	–	N	N
N2	N/18	N/10	NE/5	NE/2	NE	–	–	–	NE	NW
N3	N/65	NE/10	E/55	E/20	NE/15	NE/3	NE/1	–	NE	W–E
N4	N/4	W/2	NW/1	NW	N	–	–	–	N	NW
N5	N/2	NE/2	N/1	N	N	–	–	–	N	NNE
N6	N/2	NE/2	NW/1	NW/1	–	–	–	–	NW	NW
N7	N/3	NW/2	NW	NW	N	NNE	–	–	NNE	NW
N8	N/4	N/2	N/1	NNE/1	–	–	–	–	NNE	NE
N9	N/5	NW/4	NNW	N	N	–	–	–	N	NW
/Σ	/301	/242	/132	/57	/33	/10	/8	/2		

central and eastern segments of the Oriente fault, through an analysis of the fractability of Santiago of Cuba and Guantánamo bays, located in the central and eastern segments, respectively.

Table 11. Percentage of bifurcation index (anomalous)

Northern		Southern
BI	%	%
1–2	20	75
2–3	21	78
3–4	15	48
4–5	10	37
5–6	10	38
6–7	–	15
7–8	–	11

The Santiago de Cuba bay is located in the eastern part of the Sierra Maestra range and is adjacent to the Sierra de la Gran Piedra. It is graben, with a normal fault system and NE strike. It also has a very segmented fault with E–W strike that interrupts the prolongation north of the bay. This fault is called the Bomato. In its surrounding area there are earthquakes (two of I = 9 degrees (MSK), 11.06.1766 and 20.08.1852). However, the Guantánamo bay is not a faulting structure and has not suffered strong seismic events. Its superficial extension is greater than that of Santiago of Cuba. The seismic activity and epicentre density maps of Cotilla [12] show that the highest values are in the surrounding areas of Santiago de Cuba, to the west.

Using strike analysis of the fractures and faults, five structural zones in the Santiago Cuba bay have been identified (Fig. 13); whilst for the Guantánamo bay only three were identified. In addition, an equal quan-

Table 12. Data of the basins (see Table 9)

									Slope by maximum, %		FC_{CR}	
Basin	Fluvial terraces	Valley type	Anomalous sector	Waterfall	Lakes	Oulet type	DV, m	DH, km/km^2	Altitude	Longitude	Watershed	Main river
S1	4	U	2	1		A.L	400	0.52	8.91	8.86	1.75	1.60
S2	4	U	2	2	2	A.L	360	0.71	6.28	6.34	1.76	1.70
S3	3	U	2	2	2	A.L	290	0.70	8.78	8.73	1.78	1.70
S4	2	U			4	A.L	45	0.67	1.21	1.21	0.45	0.35
S5	5	U	1	2		A.L	100	0.80	1.50	1.50	1.48	1.50
S6	5	U	4	4	4	D.A	450	1.05	5.21	5.21	2.11	1.79
S7	6	U	5	7	4	A.L	600	1.21	13.50	13.31	2.40	2.36
S8	8	U	25	18	10	A.L	150	0.72	6.90	6.85	1.45	1.55
S9	4	U	2	2		D.A	190	1.00	7.11	6.98	1.16	1.20
S10	4	U	2	3		D.A	210	1.12	16.81	16.81	1.18	1.20
S11	3	V	4	2		D.A	190	0.71	16.71	16.71	1.11	1.16
S12	2	V	1	1		A.A	110	0.56	6.58	6.58	1.10	1.11
S13	4	V	2	2		D.A	210	0.61	3.48	3.48	1.25	1.30
S14	4	V	1	2		D.A	225	0.62	3.49	3.49	1.25	1.30
S15	5	V	4	4	2	D.A	345	1.16	15.41	15.41	1.58	1.60
S16	6	U	2	2	2	A.A	180	1.11	10.21	10.15	1.50	1.52
S17	6	V	5	6	2	A.F	248	1.16	17.10	17.10	2.00	2.00
N1	6	U	8	4	2	A.L	482	1.55	20.70	20.55	2.16	2.16
N2	5	U	2	10	4	D.A	528	1.00	20.49	20.11	1.95	1.95
N3	6	V	15	19	4	D.A	626	1.10	28.15	28.10	2.46	2.35
N4	5	U	3	2	2	D.A	200	0.80	4.72	4.70	1.01	1.01
N5	4	U	2	1		D.A	200	0.70	5.36	5.40	1.10	1.10
N6	4	U	1	2		A.A	120	0.75	5.35	5.28	1.10	1.10
N7	4	U	2	2		A.L	200	0.82	5.32	5.31	1.88	1.79
N8	4	U	2	1		A.L	190	1.32	5.00	4.95	1.78	1.68
N9	5	U	4	4	1	D.A	150	0.85	4.71	4.65	1.55	1.51
Σ	118	U = 19, V = 7	103	105	45							

Note: A.L –acumulative of the bay and lake type; A.F—abrasive and faulting type; A.A—plain and abrasive type; D.A—rough and abrasive type; FC_{CR}—factor of significant slope change in the watersheds and rivers.

Table 13. Some fluvial parameters (see Table 9)

Basin	IS_{cf}/IAS_{cf}	IF_{cf}/IO_{cf}	F_{cec}	IPEF	I_{ai}	I_{ol}
S1	0.40	1.81	0.91	1.1	1.1	0.79
S2	0.42	2.0	0.88	1.2	1.1	0.77
S3	0.40	2.26	0.88	1.7	1.3	0.78
S4	0.42	1.5	0.40	1.6	0.4	0.80
S5	0.51	2.3	0.67	2.1	2.0	0.83
S6	0.55	2.3	0.81	3.2	2.5	0.80
S7	0.63	3.6	0.92	3.4	2.9	0.90
S8	0.63	4.1	090	3.7	2.8	0.77
S9	0.40	4.2	0.92	2.2	1.2	0.83
S10	0.47	4.0	0.92	2.1	1.3	0.88
S11	0.40	3.5	0.86	1.8	1.5	0.60
S12	0.31	4.7	0.76	1.6	1.5	0.95
S13	0.32	4.6	0.75	1.9	1.8	0.90
S14	0.41	4.7	0.75	1.8	1.8	0.90
S15	0.33	3.1	0.70	2.3	2.0	0.78
S16	0.50	3.9	0.71	3.0	1.7	0.90
S17	0.47	4.0	0.81	3.2	2.0	0.93
N1	0.44	3.9	0.92	3.2	2.7	0.90
N2	0.39	3.1	0.92	2.9	2.7	0.78
N3	0.48	3.7	0.95	3.9	3.1	0.81
N4	0.27	1.26	0.67	1.3	1.2	0.38
N5	0.41	1.76	0.70	1.1	1.1	0.72
N6	0.45	2.0	0.67	1.1	1.1	0.81
N7	0.43	2.2	0.79	2.7	1.4	0.67
N8	0.40	2.0	0.77	2.2	1.2	0.65
N9	0.50	3.5	0.77	2.0	1.9	0.80

Note: IS_{cf}/IAS_{cf}—the symmetry/asymmetry index of the fluvial basins along their divides and along meir fluvial channels; IF_{cf}/IO_{cf}—the index of the shape and orientation of the basins; F_{cec}—the factor of the visual change of the basins; IPEF—the potential intensity of fluviaferosion; I_{ai}—the elevation/number of intersection of rivers index; I_{ol}—the orientation/length of river index.

tity of stress models were obtained, using the proposal of Wice et al. [88]. The fractal dimensions obtained with the box-counting technique using various minimal scales, for the two studied zones, are high (Table 14). This is considered to be due to the fact that horizontally, the fracture network is very extended, but not uniform. The values of the fractal dimension established for the two basins (Santiago of Cuba (D = 1.98) and Guantanamo (D = 1.47)) agree with the geometric structure of the fracturation analyzed without exceeding the stated condition of the value 2.0. These data bear a direct relation to seismic activity levels and M_{max} earthquake value Cotilla [12] also showed that focal mechanisms are different from east to west in Santiago de Cuba. In Figure 5 [15], this differentiation can be clearly observed.

It is important to mention that Sukmono et al. [80] asserted that larger values for D are associated with more complicated fault geometry. Other authors also arrived at similar results, among them T. Hirata [44] found D ≈ 1.05–1.60 for Japan; Konkouvelas et al. [55] found D ≈ 1.0 for Greece. Along the same lines of research, S. Sukmono [78], Sukmono et al. [79] suggested that there is a repetitive pattern (or fractal pattern of the Sumatra fault system) and found D ≈ 1.0–1.21. This latter can be deduced from the results of P.G. Silva [76] for the Lorca–Alhama fault, in Spain. Thus, the results obtained for Santiago de Cuba and Guantánamo are very reliable.

Finally, the fractal dimension value in the case of the Cauto river (S8), taking the interval for logL to be between 2.55 and 3.5 (when the correlation coefficient is very significant, r = 0.999) is D = 1.77. Since this dimension differs from 1 to 2, assuming higher values given that the structural influence is stronger, with a fractal dimension of 1.77 it is highly probable that the evolution of the Cauto river has been strongly conditioned by tectonics.

CONCLUSIONS

Using accurate field work mostly based on topographic maps, aerial photographs and Cuban geological projects it can be asserted that neotectonics, as an endogenous process, has influenced and continues to influence Cuban relief types. This is a topographically emerged structure in the south of the North American plate, demonstrated by the line of coast (geometry and correlated structures), the mountain ranges (altitude, disposition and geometry), sediment deposits (fans and cones), slope ruptures (scarps and waterfalls), the fluvial system, and the intensity of vertical and horizontal movements. In particular it has been confirmed that river geometry is conditioned by these processes. All of the higher order streams follow a general structural trend indicating that drainage in the Cuba megablock is structurally controlled.

The fractures identified in the 26 selected areas of Cuban territory were subjected to statistical treatment using GIS. In general, they are associated with several active faults. There is a marked differentiation with regard to the fracturing of the Oriente fault northern segment in Southeastern Cuba. In addition, the Santiago de Cuba and Guantánamo basins, although close to the Oriente fault, have different morphologic and morphometric characteristics, and the nine karstic areas studied show significant differences in terms of fracturing.

The Oriente fault (segment of the North American–Caribbean plate boundary) can be divided into two segments, in the line between Cabo Cruz and Punta de Maisí, (Western and Eastern), on the basis of a set of thirteen neotectonic characteristics of seismicity and

Table 14. Fractal analysis

	Bays	
	Santiago de Cuba	Guantánamo
Calculation method	frequency	frequency
Closs interval	5°	5°
Data type	Bidimensional	Bidimensional
Rotation amount	0°	0°
Population	1.046	535
Maximum percentage	10.1%	25.4%
Mean percentage	2.5%	4.2%
Standard deviation	2.0%	3.65%
Confidence interval	6.98°	6.12°
Fractal dimension (D)	1.98	1.47

focal mechanisms. This differentiation is also indirectly supported by a fractal analysis of the Santiago de Cuba (1.98) and Gauntánamo (1.47) bays. This agrees reliably with levels of seismic activity and maximum earthquake magnitudes.

The Nortecubana fault, on the northern limit of the Cuban megablock is divided into three segments: Cabo de San Antonio—Punta de Hicacos, Punta de Hicacos—Cauto–Nipe, and Cauto–Nipe—Punta de Maisí in terms of seismicity and the strike of the principal fracture. The most active of them is the central one.

The Cauto–Nipe fault, forming the limit of the neotectonic units (Western and Eastern), has two segments and comprises three seismoactive knots (Cabo Cruz, San Germán, Banes–Nipe). In addition, this fault has facilitated the development a pull-apart basin in the surroundings of the Bayamo–Manzanillo.

ACKNOWLEDGMENTS

The research was carried out in the Geophysics and Meteorology Department of the Physical Sciences Faculty of the Complutense University of Madrid. Financial backing came, in part, from the Comunidad de Madrid (post-doctoral grant for 2001–2004). This paper is a contribution to REN2003–08520-C02-02, REN2002-1249E/RIES and CGL2005–25012-E projects.

For the colaboration of Prof. Armando Cisternas (Institute du Physique du Globe, Strasbourg) in the fractal study. The first author wishes to thank the following experts for their help on our field trips: 1) Cuba: Enio C. González, Guillermo Millán, and Humberto Álvarez (Instituto de Geología y Paleontología); Leandro Llanes (Facultad de Geografía); Mario Campos (Instituto de Geofísica y Astronomía); and Bárbara Fernández (Centro Nacional de Investigaciones Sismológicas); 2) Germany: Joachim Pilarski and Joachim Franzke.

REFERENCES

1. *Academia de Ciencias de Cuba. Levantamiento geológico de las provincia habaneras, escala 1 : 250000, 1981a*, Archivo del Instituto de Geología y Paleontología [in Spanish].
2. *Academias de Ciencias de Cuba y de Bulgaria. Levantamiento geológico de Las Villas, escala 1 : 250000, 1981b*, Archivo del Instituto de Geología y Paleontología [in Spanish].
3. *Academias de Ciencias de Cuba y de Bulgaria. Levantamiento geológico de Ciego de Avila, Camagüey y Las Tunas, escala 1 : 250000, 1981c,* Archivo del Instituto de Geología y Paleontología [in Spanish].
4. *Academias de Ciencias de Cuba y de Hungria. Levantamiento geológico de las provincias Orientals, escala 1 : 250000, 1981d*, Archivo del Instituto de Geología y Paleontología [in Spanish].
5. *Academias de Ciencias de Cuba y de Polonia. Levantamiento geológico de Matanzas, escala 1 : 250000, 1981e*, Archivo del Instituto de Geología y Paleontología [in Spanish].
6. *Academias de Ciencias de Cuba y de Polonia. Levantamiento geológico de Pinar del Río, escala 1 : 250000, 1978*, Archivo del Instituto de Geología y Paleontología [in Spanish].
7. Yu. M. Arseniev, G. Capote, and S. N. Kalashov, *Esquema cosmofotectónico de Cuba, escala 1 : 500000* (Informe del Centro Nacional de Investigaciones Geológicas, Ministerio de la Industria Básica, 1983), p. 25 [in Spanish].
8. P. Bankwitz, F. K. List, Eds., *Proceedings of the Third United Nations International Training Course on Remote Sensing Applications to Geological Science*, Vol. 1: *Berliner geowiss*, Abh. D, 1992, p. 155.
9. G., Barceló, B. E. González, M. O. Cotilla, and T. Chuy, "Análisis del fracturamiento de la región de Santiago de Cuba," Revista Ciencias de la Tierra y del Espacio **8**, 11–27 (1984) [in Spanish].
10. R. Brino and G. Raspa, "Geostatistical characterization of fractals models of surfaces," Geostatistics **1**, 77–89 (1989).
11. M. O. Cotilla, "An overview on the seismicity of Cuba," Journal of Seismology **2**, 323–325 (1988a).
12. M. O. Cotilla, "Empleo de la fotointerpretación de materiales aéreos multizonales en la identificación de fracturas en un sector del Gran Parque Nacional Sierra Maestra," Comunicaciones Científicas sobre Geofísica y Astronomía **9**, 16 (1988b) [in Spanish].
13. M. O. Cotilla, "Estudio geomorfológico complejo de un sector del norte de Holguín para las investigaciones de microrregionalización sísmica de la Central Electronuclear," Comunicaciones Científicas sobre Geofísica y Astronomía **12**, 25 (1988c) [in Spanish].
14. M. O. Cotilla, *Una caracterización sismotectónica de Cuba. PhD Thesis, Instituto de Geofisica y Astronomía* (Academia de Ciencias de Cuba, 1993), p. 200 [in Spanish].
15. M. O. Cotilla, "Estudio geomorfológico del carso en la región Gibara-Banes, Holguín, Cuba," Revista Geográfica **134**, 5–22 (2003) [in Spanish].

16. M. O. Cotilla and J. L. Álvarez, "Regularidades sismogenéticas de la unidad neotectónica Occidental de Cuba," Revista Geológica de Chile **28** (1), 3–24 (2001) [in Spanish].
17. M. O. Cotilla and D. Córdoba, "Present geomorphological characterisitics of Alboran Islet and surroundings, Spain: a diagnosis," Geogr. Fis. Dinam. Quat. **27**, 3–19 (2004).
18. M. O. Cotilla and H. J. Franzke, "Some comments on the seismotectonic activity of Cuba," Z. Geol. Wiss. **22** (No. 3/4), 347–352 (1994).
19. M. O. Cotilla, T. Chuy, and L. Llanez, *Caracterización neotectónica de un sector del norte de Holguín para la Central Electronuclear*, (Informe de la Academia de Ciencias de Cuba, 1983), p. 25 [in Spanish].
20. M. Cotilla, E. San Martín, F. Arteaga, and M. Gónzalez, *Empleo de la fotointerpretación de materiales aerocósmicos para la identificatión de fracturas en la Sierra Maestra*, (Informe del Instituto de Geofísica y Astronomía, 1985), p. 20 [in Spanish].
21. M. Cotilla, H. J. Franzke, J. Pilarski, M. Pilarski, and L. Álvarez, "Mapa de alineamientos y nudos tectónicos rpincipales de Cuba, a escala 1 : 1000000," Revista de Geofísica **35**, 53–112 (1991a) [in Spanish].
22. M. O. Cotilla, E. C. Gónzalez, H. J. Franzke, J. L. Díaz, F. Arteaga, and L. Álvarez, "Mapa neotectónico de Cuba escala 1 : 1000000," Comunicaciones Cientificas sobre Geofísica y Astronomía **22**, 37 (1991b) [in Spanish].
23. M. O. Cotilla, C. Cañete, R. Carral, J. L. Díaz, R. Pérez, and C. Pérez, *Esquema de alineamientos principales de la región Cochinox–Tunas, a escala 1 : 50000*, (Informe de la Academia de Ciencias de Cuba y del Ministerio de la Industria Básica, 1992), p. 100 [in Spanish].
24. M. Cotilla, G. Millán, L. Álvarez, D. Gónzalez, M. Pacheco, and F. Arteaga, *Esquema neotectogénico de Cuba,* Informe científico-técnico del Departamento de Geofísica del Interior, 1996), p. 100 [in Spanish].
25. M. O. Cotilla, L. Díaz, D. Gónzalez, M. Fundora, and M. Pacheco, "Estudio morfoestructural de La Española," Revista Mineria y Geología **14** (3), 73–88 (1997) [in Spanish].
26. M. O. Cotilla, E. C. Gónzalez, C. C. Cánete, J. L. Díaz, and R. Carral, "La red fluvial de Cuba y su interpretación morfoestructural," Revista Geográfica **134**, 47–74 (2003) [in Spanish)].
27. R. T. Cox, "Análisis of drainage basin symmetry as a rapid technique to identify areas of possible Quaternary tilt-block tectonics: an example from the Missisippi embaymen," Geol. Soc. Am. Bull. **106**, 571–581 (1994).
28. A. P. Dedrov, *Sobre el vínculo del orden y la edad de los valles fluviales* (Editorial Universidad de Kazan, URSS, 1966) [in Russian].
29. M. del Monte, P. Fredi, E. Lupia Palmieri, and F. Salvani, "Fractal analysis to define the drainage network geometry," Bull. Soc. Geol. It. **118**, 167–177 (1999).
30. J. L. Díaz, *Morfoestructuras de Cuba Occidental. Ph. Thesis*, (Academia de Ciencias de la URSS, 1985), p. 200 [in Russian].
31. A. A. Ferens-Sorotskig, P. N. Satranov, and V. I. Alakzeen, "Configuración de la red hidráulica, como indice de los movimientos tectónicos locales en la parte norte de la depresión del Pichora," Revista Geomorfología, **4**, 52–57 (1972) [in Russian].
32. V. P. Filosofov, *Manual breve de búsqueda de las estructuras tectónicas por el método morfométrico* (Editorial Nedrá, Moscú, 1960) [in Russian].
33. V. P. Filosofov, *Metodología para el calculo e interpretación geólogica y geomorfológica del coeficiente de desmembramiento del relieve en cuestiones de morfometría* (Editorial Nedrá, Moscú, 1967a) [in Russian].
34. V. P. Filosofov, *Sobre la importancia del orden de los valles y de las líneas divisorias de aguas durante las investigaciones geomorfológicas* (Universidad de Saratov, URSS, 1967b) [in Russian].
35. V. P. Filosofov, *Vínculo de los órdenes de los valles y divisorias de aguas con su edad geológica en el territorio de Saratov, junto al Volga* (Universidad de Saratov, URSS, 1967) [in Russian].
36. G. García, "Esquema morfoestructural de la cuenca del Cauto según datos morfométricos y de teledetección," Revista Minería y Geología **12** (3), 33–38 (1995) [in Spanish].
37. E. Gónzalez, C. Cañete, J. Díaz, L. Pérez, M. Cotilla, "Esquema neotectónico de Cuba, escala 1 : 250000," Revista Serie Geológica, **1**, 16–34 1989 [in Spanish].
38. E. C. Gónzalez, M. O. Cotilla, C. C. Cañete, J. L. Díaz, *Esquema geomorfólogo-estructural de la Sierra Maestra, escala 1 : 1000000. Informe Final del Proyecto de Metalogenia de la Sierra Maestra, Capítulo Geomorfología y Neotectónica* (Instituto de Geología y Paleontologia, Ministerio de la Industria Básica, 1990), p. 200 [in Spanish].
39. E. C. Gónzalez, M. O. Cotilla, C. C. Cañete, J. L. Díaz, R. Carral, and F. Arteaga, "Estudio morfoestructural de Cuba. Geogr.," Fis. Dinam. Quat. **26** (1), 49–70 (2003) [in Spanish].
40. J. Hack, "Stream profile analysis and stream gradient index," U.S. Geol. Survey J. Res. **1**, 421–429 (1973).
41. J. R. Hernández, R. Gónzalez, A. Venereo, and J. Avila, "Estudio de los procesos fluviales de cauce recientes del río Carpintero (Cuba), mediante métodos geodésicos," Ciencias de la Tierra y del Espacio **10**, 39–55 (1987) [in Spanish].
42. J. R. Hernández, P. Blanco, J. L. Díaz, *Rasgos estructuro-geomorfológicos del fondo de los mares ó océanos circundantes a Cuba* (La Habana: Editorial Academia, 1988), p. 14 [in Spanish].
43. J. R. Hernández, J. L. Díaz, O. Bouza, and R. Gónzalez, "Influencia de las particularidades morfoestructurales de Cuba Sudoriental en la forma de los valles y terrazas fluviales," Reporte de Investigación del Instituto de Geografía **2**, 20 (1989) [in Spanish].
44. T. Hirata, "Fractal dimension of fault systems in Japan: fractal structure in rock fracture geometry at various scales," Pure appl. geoph. **131** (1/2), 157–170 (1989).
45. R. E. Horton, "Drainage basin characteristics," Trans. Amer. Geophys. Union. **13**, 350–361 (1932).
46. R. E. Horton, "Erosional development of streams and their drainage basins, hydrological approach to quantitative morphology," Geol. Soc. Am. Bull. **56**, 275–370 (1945).

47. A. D. Howard, "Drainage analysis in geologic interpretation: a summation," Bull. Am. Assos. Petroleum Geologists **51**, 2246–2259 (1967) .
48. *Fotos aéreas de Cuba, escala 1 : 62000*, (Instituto Cubano de Geodesia y Cartografía [ICGC], 1956).
49. *Fotos aéreas de Cuba, escala 1 : 37000,* (Instituto Cubano de Geodesia y Cartografía [ICGC], 1982).
50. *Mapas topográficos de Cuba, escala 1 : 250000*, (Instituto Cubano de Geodesia y Cartografia [ICGC], 1986a).
51. *Mapas topográficos de Cuba, escala 1 : 50000,* (Instituto Cubano de Geodesía y Cartografía [ICGC], 1986b.
52. *Mapas topográficos de Cuba, escala 1 : 10000,* (Instituto Cubano de Geodesía y Cartografía [ICGC], 1988).
53. M. Iturralde, "Cuban geology: A new plate-tectonic synthesis," Jour. Petrol. Geol. **17** (1), 59–10 (1992).
54. F. Kohlbeck and A. E. Scheidegger, "On the theory of the evaluation of joint orientation measurements," Rock Mech. **9**, 9–25 (1977).
55. I. K. Konkouvelas, M. Asimakopoulos, and T. T. Doutsos, "Fractal characteristics of active normal faults: an example of the eastern gula of Corinth, Greece," Tectonophysic **308**, 263–274 (1999).
56. G. Korvin, *Fractal models in the Herat sciences* (Elsevier, Amsterdam, 1992).
57. S. S. Korzhuev, "Estudio del diseño general de la red fluvial," *Análisis morfoestructural de la red fluvial de la URSS* (Editorial Nauka, Moscu, 1979), pp. 5–9 (in Russian).
58. L B. Leopold and M. G. Wolman, "River channel patterns: braided, meandering, and straight," U.S. Geol. Survey Prof. Paper **28** L-B (1957).
59. E. Linares, A. V. Dovbnia, P. G. Osadchiy, P. G. Judoley, S. Gil, D. Garcia, and A. Zuazo, G. Furrazola, A. Brito, Y. B. Evdokimov, B. A. Markovskii, V. A. Trofimov, A. L. Vtulockkin, *Mapa geológico de Cuba, escala 1 : 500000,* (Centro de Investigaciones Geológicas, Ministerio de la Industria Básica de Cuba, 1986).
60. F. K. List and P. Bankwitz, Eds., *Proceedings of the Fourth United Nations. CDG International Training Course on Remote Sensing Applications to Geological Sciences.* (Berliner geowiss. Abh. D, 1993), Vol. 5, p. 119.
61. B. B. Malderbrot, "How long is the coast of Britain? Statistical self-similarity and fractional dimension," Science **156**, 636–638 (1967).
62. B. B. Malderbrot, *Self affine fractal sets I, II, II. Fractals in Physics.* Eds. by L. Pietronero and E. Tasatti (Elsevier Science Publishers, 1986).
63. D. Merrits and T. Herterbergs, "Stream networks and long term surface uplift in the New Madrid seismic zone," Nature **265**, 1081–1084 (1994).
64. A. Mossakovsky, Y. Pusharovskii, G. E. Nekrasov, S. R. Sokolov, F. Formel, R. Cabrera, M. Iturralde, R. Flores, J. Oro, A. Morales, G. Pantaleón, L. Perez, A. Pszozolkowski. et al., *Mapa tectónico de Cuba, escala 1 : 50000,* (Instituto de Geologia y Paleontologia, Academia de Ciencias de Cuba, 1989).
65. P. G. Okubo and K. Aki, "Fractal geometry in the San Andreas fault system," J. Geophys. Res. **92**, 345–355 (1987).
66. C. Pérez, J. Oro, F. Formel, L. Pérez, V. G. Trifonov, and G. V. Makarov, *Aplicación de la teledetección en le estudio de la geología de Cuba. Informe Final del Tema 314.10* (Instituto de Geología y Paleontologia, Academia de Ciencias de Cuba, 1985) [in Spanish].
67. A. Portela, P. Blanco, J. Díaz, and A. Magaz, *Alineamientos y estructuras circulares en la imagen cósmica del Landsat de a parte occidental de la provincia de Pinar del Río. Informe del Instituto de Geografía* (Academia de Ciencias de Cuba, 1981 (in Spanish).
68. A. Rodriguez and J. Blanco, "Fallas de deslizamiento por el rumbo en la región de Moa," Revista Minería y Geología **18** (1), 45–48 (2000) [in Spanish].
69. A. Rodríguez, M. Mundi, and J. L. Castillo, "Morfotectónica y sismotectónica de la región de Moa," Revista Minería y Geología **13** (2), 13–16 (1996) [in Spanish].
70. A. Rodríguez, N. Camacho, and M. Conde, "Estudio de las estructuras sismogeneradoras Exigua y El Medio, al este de la Ciudad de Moa," Revista Minería y Geología **17** (3–4), 87–90 (2000) [in Spanish].
71. M. I. Ross and Ch. Scotese, "A hierarchical tectonic model of the Gulf of Mexico and Caribbean region," Tectonophysics **15**, 139–168 (1988).
72. A. E. Scheidegger, "Joints as neotectonic plate signatures," Tectonophysics **219**, 235–239 (1993).
73. S. A. Schumm, J. F. Dumont, and J. M. Holbrook, *Active tectonics and alluvial rivers* (Cambridge: Cambridge University Press, 2000), p. 276.
74. V. S. Shein, K. A. Klishov, V. E. Jain, G. E. Dikenshtein, J. L. Yparraguirre, E. García, and R. Rodríguez, *Mapa tectónico de Cuba, escala 1 : 500000*, (Centro de Investigaciones Geológicas, Ministerio de la Industria Básica de Cuba, 1985).
75. R. L. Shreve, "Statistical law of stream numbers," J. Geology **74** 17–37 (1966).
76. P. G. Silva, "Geometría fractal de la zona de falla de Lorca–Alhama (Murcia, SE España)," Geogaceta **20** (6) 1.385–1.388 (1996) [in Spanish].
77. A. N. Strahler, "Quantitative analysis of watershed geomorphology," Annals. Geophys. Union Trans **38** (6), 913–920.
78. S. Sukmono, "New evidence on the fractal pattern of Sumatra fault seismicity and its possible application to earthquake prediction," Bull. Seism. Soc. Am. **91** (4), 870–874 (2001).
79. S. Sukmono, M. T. Zen, G. A. Kadir, L. Hendraya, D. Santoso, and J. Dubois, "Fractal geometry of the Sumatra active fault system and its geodynamical implications," J. Geodynamics, **22** (1/2), 1–9 (1996).
80. S. Sukmono, M. T. Zen, L. Hendraya, W. G. A. Kadir, D. Santoso, and J. Dubois, "Fractal pattern of the Sumatra fault seismicity and its possible application to earthquake prediction," Bull. Seism. Soc. Am. **87** (6), 1685–1690 (1997).
81. S. Taber, "The structure of the Sierra Maestra near Santiago de Cuba," J. Geology **39**, 532–557 (1931).
82. A. Thomas, "Structure fractale de l'architecture de champu de fractures en milieu rocheux," Comptes. Rendus Academy Science Paris **2** (4), 181–186 (1987) [in French].
83. V. D. Trifonov, F. Formel, J. Oro, and C. Pérez, *Mapa de elementos estructurales de la provincia de Oriente*

(Informe del Instituto de Geología y Paleontología, Academia de Ciencias de Cuba, 1981a) [in Spanish].

84. V. D. Trifonov, F. Formel, J. Oro, and C. Pérez, *Mapa de elementos estructurales de la provincia de Pinar del Río* (Informe del Instituto de Geología y Paleontología, Academia de Ciencias de Cuba, 1981b) [in Spanish].

85. D. L. Turcotte, *Fractals and chaos in Geology and Geophysics* (Cambridge: Cambridge University Press, 1992).

86. J. G. Vedder and R. E. Wallace, *Map showing recently active breaks along the San Andreas and related faults between Cholame Valley and Tejon Pass, California, scale 1 : 24000* (U.S. Geol. Suv. Misc. Geol. Inv. Map., 1–154, 1970).

87. J. J. Walsh and J. Watterson, "Fractal analysis of fracture patterns using the standard box-counting technique: valid and invalid methodologies," J. Struct. Geol. **15** (12), 1509–1512 (1993).

88. D. Wice, R. Funcielio, M. Porotto, and F. Salvani, "Features and lineament orientations in Haly," Geol. Soc. Am. Bull. **96**, 112–138 (1985).

89. E. R. Zennitz, "Drainage patterns and their significance," J. Geology **40**, 498–521 (1932).

Reviewer: V. G. Trifonov